

# AGA5802

## Prism spectroscopy

- Introduction
- Basic information about design of spectrographs
- *Prism spectrographs*
- *Applications*

*Bibliography: To Measure the Sky, Kitchin, Lena and others, like a book by C. Kitchin specifically on Optical Astronomical Spectroscopy (on line formation and instrumentation)*

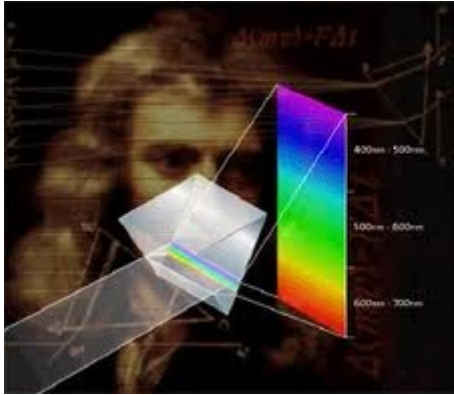


In 1835, the French philosopher Auguste Comte, considered the limits of human knowledge. He thought that the chemical composition of the stars was a prime example of "unobtainable knowledge":

Why?

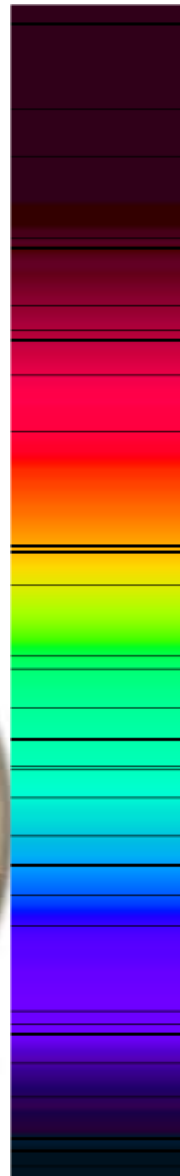
On the subject of stars, all investigations which are not ultimately reducible to simple visual observations are ... necessarily denied to us ... **We shall never be able by any means to study their chemical composition**

# Continuous (optical) spectrum



Newton (1666)

# Line spectrum



Joseph von Fraunhofer (1787-1826)

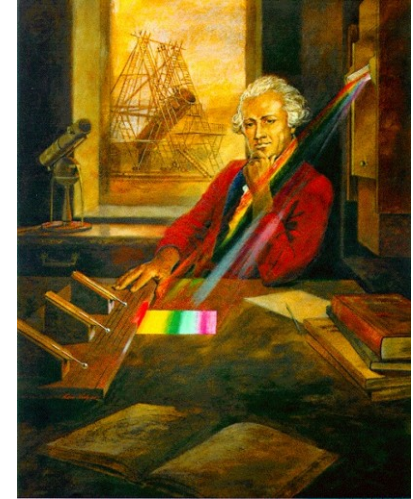
Fraunhofer (1817)

574 lines

Better prism + slit

# Infrared spectrum

William Herschel (1800)



William Hyde Wollaston (1766-1828)

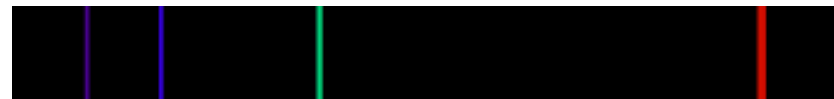
Wollaston

(1802)

7 lines

# Emission spectrum

John Herschel (son of William) and William Henry Fox Talbot, 1820s



# A Method of Examining Refractive and Dispersive Powers, by Prismatic Reflection

PHILOSOPHICAL

William Hyde Wollaston

TRANSACTIONS:

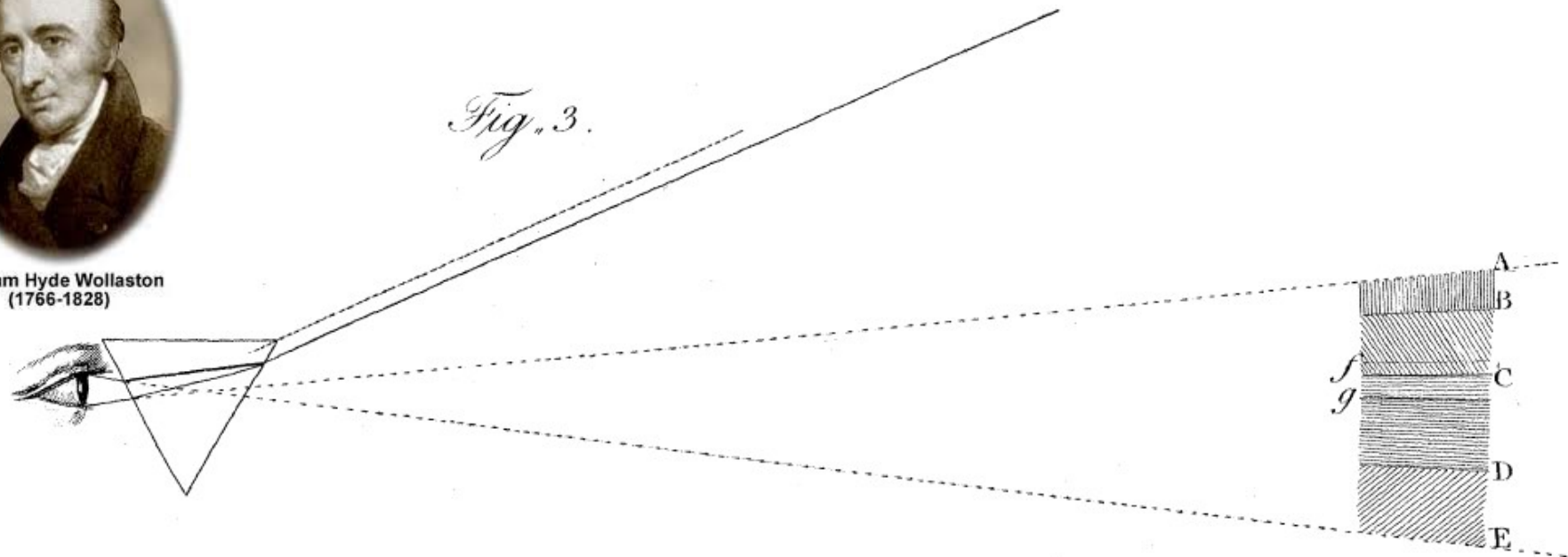
*Phil. Trans. R. Soc. Lond.* 1802 **92**, doi: 10.1098/rstl.1802.0014, published 1 January 1802

I cannot conclude these observations on dispersion, without remarking that the colours into which a beam of white light is separable by refraction, appear to me to be neither 7, as they usually are seen in the rainbow, nor reducible by any means (that I can find) to 3, as some persons have conceived; but that, by employing a very narrow pencil of light, 4 primary divisions of the prismatic spectrum may be seen, with a degree of distinctness that, I believe, has not been described nor observed before.

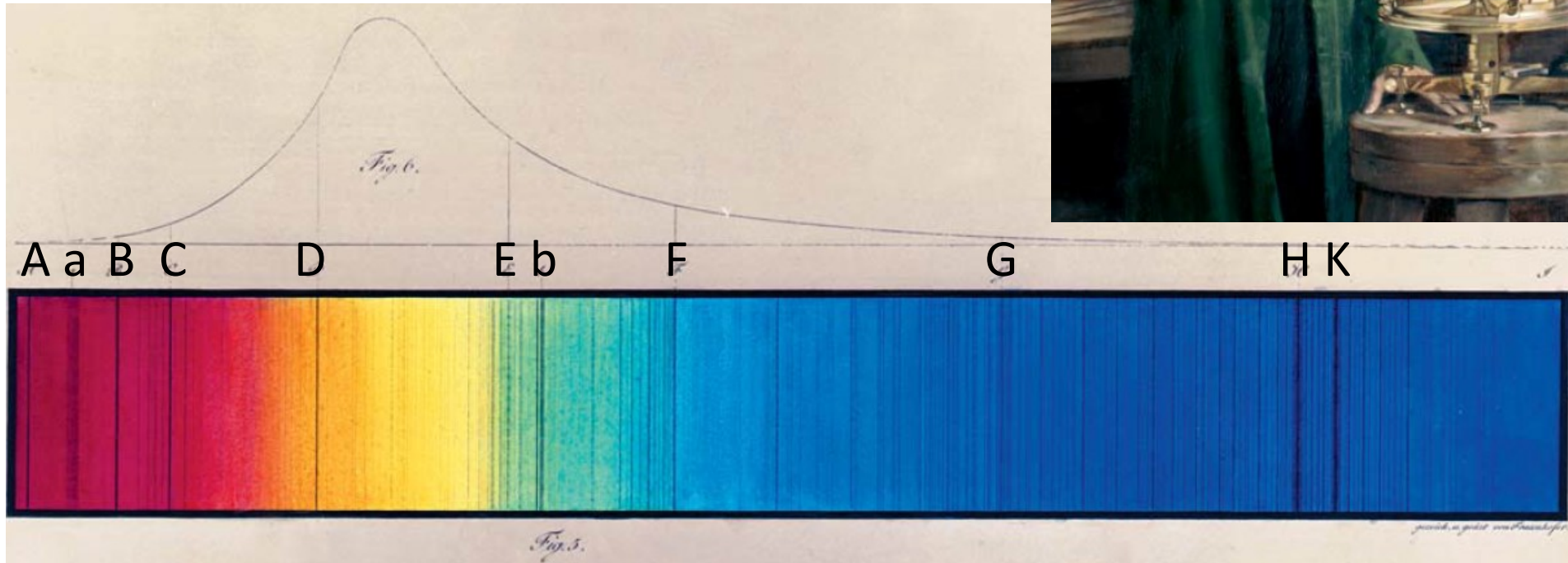
The line A that bounds the red side of the spectrum is somewhat confused, which seems in part owing to want of power in the eye to converge red light. The line B, between red and green, in a certain position of the prism, is perfectly distinct; so also are D and E, the two limits of violet. But C, the limit of green and blue, is not so clearly marked as the rest; and there are also, on each side of this limit, other distinct dark lines, *f* and *g*, either of which, in an imperfect experiment, might be mistaken for the boundary of these colours.



William Hyde Wollaston  
(1766-1828)



# Fraunhofer found 574 lines in the solar spectrum (1817)



O<sub>2</sub> O<sub>2</sub> H $\alpha$  Na Fe Mg H $\beta$  CH Ca I  
H<sub>2</sub>O  
Earth

# DENKSCHRIFTEN

DER

RÖNIGLICHEN

AKADEMIE DER WISSENSCHAFTEN

ZU MÜNCHEN

FÜR DIE JAHRE

1814 UND 1815.



Joseph von Fraunhofer  
(1787-1826)

## Bestimmung

des

Brechungs- und Farbenzerstreuungs-Vermögens

verschiedener Glasarten,

in

Bezug auf die Vervollkommnung achromatischer

Fernröhre.

Von

Joseph Fraunhofer,

Fraunhofer,  
father of  
astronomical  
spectroscopy

Joseph Fraunhofer (1814 - 1815), in *Denkschriften der Königlichen Akademie der Wissenschaften zu München*

Ich habe auch mit derselben Vorrichtung Versuche mit dem Lichte einiger Fixsterne erster Größe gemacht. Da aber das Licht dieser Sterne noch vielmal schwächer ist, als das der Venus, so ist natürlich auch die Helligkeit des Farbenbildes vielmal geringer. Demohngeachtet habe ich, ohne Täuschung, im Farbenbilde vom Lichte des Sirius drey breite Streifen gesehen, die mit jenen vom Sonnenlichte keine Aehnlichkeit zu haben scheinen; einer dieser Streifen ist im Grünen, und zwey im Blauen. Auch im Farbenbilde vom Lichte anderer Fixsterne erster Größe erkennt man Streifen; doch scheinen diese Sterne, in Beziehung auf die Streifen, unter sich verschieden zu seyn.

With the same device [i.e., spectroscope], I've also made some experiments on the light of some stars of the first magnitude. Since the light of these stars is many times weaker than that of Venus, so naturally the brightness of the spectrum is also many times less.

Notwithstanding, **I have seen -- without any illusion -- three broad stripes in the spectrum of Sirius, which seem to have no similarity to those of sunlight; one of these stripes is in the green, and two in the blue. Also, in the spectrum of the light of other fixed stars of the first magnitude, one detects stripes; yet these stars, in regard to the stripes, seem to differ among themselves.**



William Huggins, 7 Feb 1824 – 12 May 1910.

~1860 Gustav Kirchhoff identified sodium in the Sun

- 1862 Anders Ångström identified hydrogen in the Sun

- 1864 W. Huggins identified H, Fe, Na and Ca in stars

He also studied the spectra of comets and nebulae

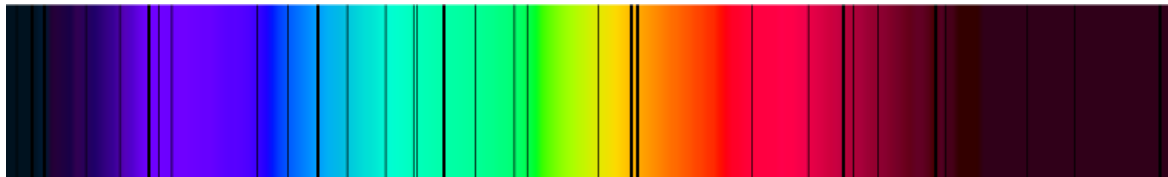


He built his own instruments and introduced a comparison “laboratory” spectrum to determine precisely the wavelengths of stars.

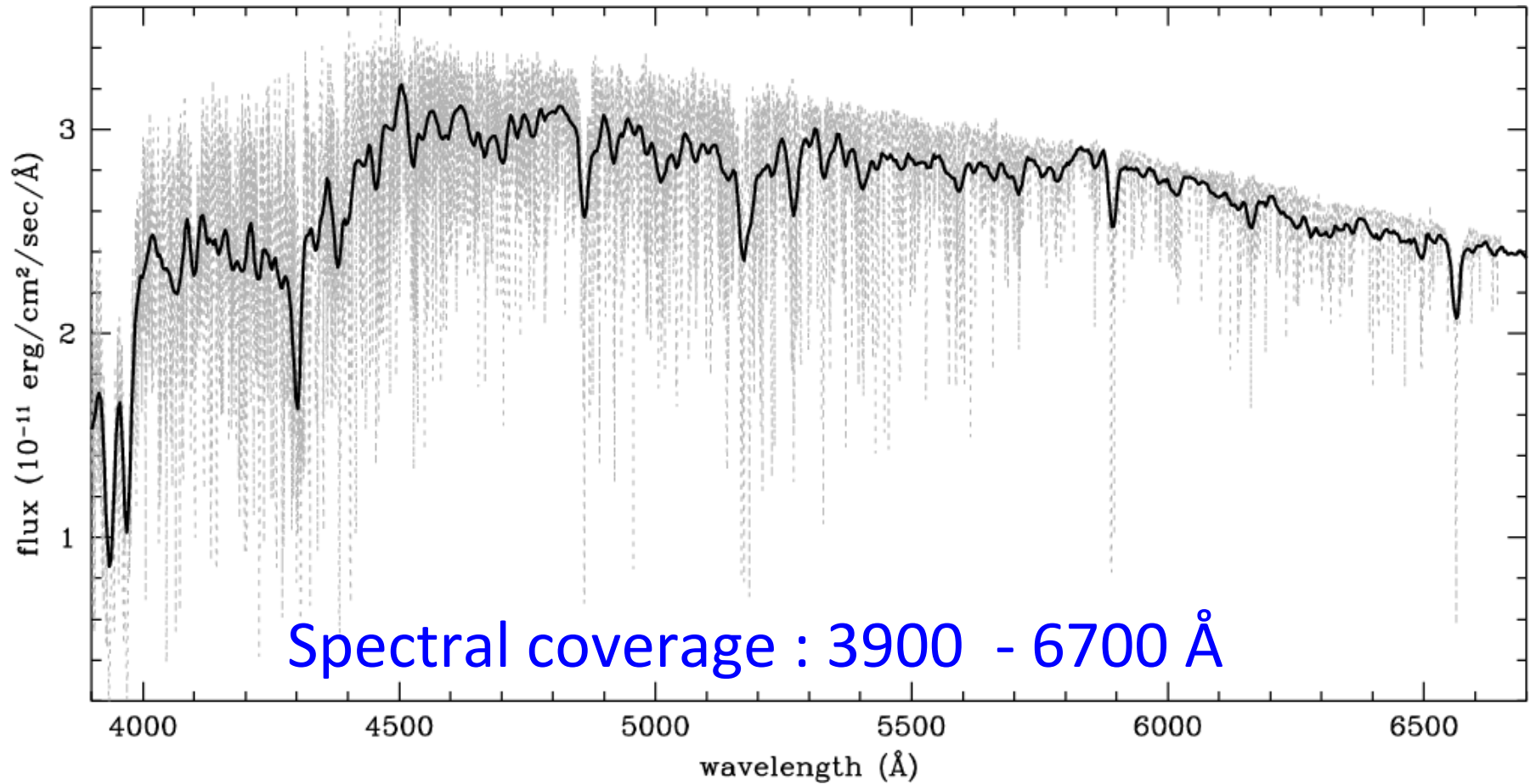
1868: Radial velocity of Sirius

# Characteristics of spectra

- Wavelength  $\lambda$  ,frequency  $\nu$  ou velocity  $v$
- Spectral resolution:  $\Delta\lambda$ ,  $\Delta\nu$ ,  $\Delta v$   
 $\Delta\lambda$ ,  $\Delta\nu$ ,  $\Delta v$  : spectral resolution element in wavelength, frequency or velocity
- Resolving power : R  
 $R = \lambda/\Delta\lambda$ ,  $R = \nu/\Delta\nu$ ,  $R = c/\Delta v$
- Spectral coverage :  $\lambda_{\min} - \lambda_{\max}$



Low spectral resolution ( $\Delta\lambda \geq 1 \text{ \AA}$ ) vs.  
High spectral resolution ( $\Delta\lambda \sim 0,1 \text{ \AA}$ )



# A water vapour maser in the Large Magellanic Cloud

E. Scalise Jr

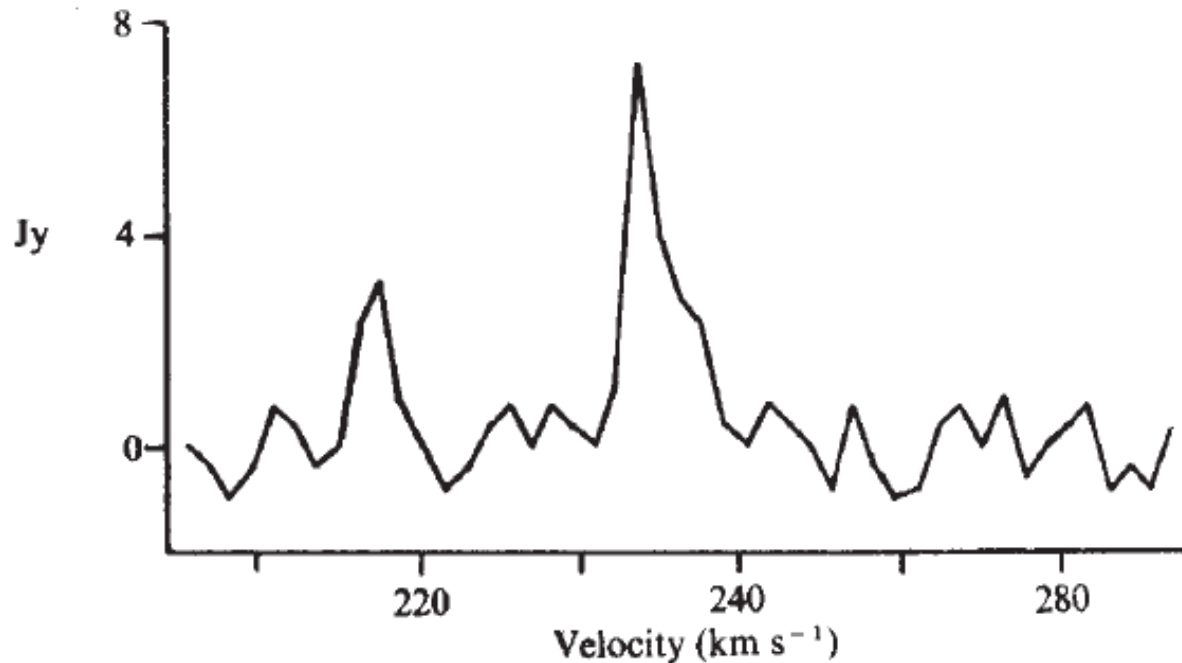
CRAAM/INPE: Instituto de Pesquisas Espaciais, Conselho Nacional de Desenvolvimento, Científico e Tecnológico-CNPq, CP 515, 12200-São José dos Campos, SP, Brasil

M. A. Braz

CNPq-Observatório Nacional, Rua Pará, 277, 01243-São Paulo, SP, Brasil

The survey was carried out in 1979-80. Upper detection limits of about 1.2 Jy were attained with the use of long integration times and a maser amplifier front-end, the total system temperature ranging from 250 to 400 K. Spectral information was provided by a 47-channel spectrometer, 100-kHz bandwidth filter bank, giving a velocity resolution of  $1.35 \text{ km s}^{-1}$ . Two vertically polarized feed horns were used in beam-

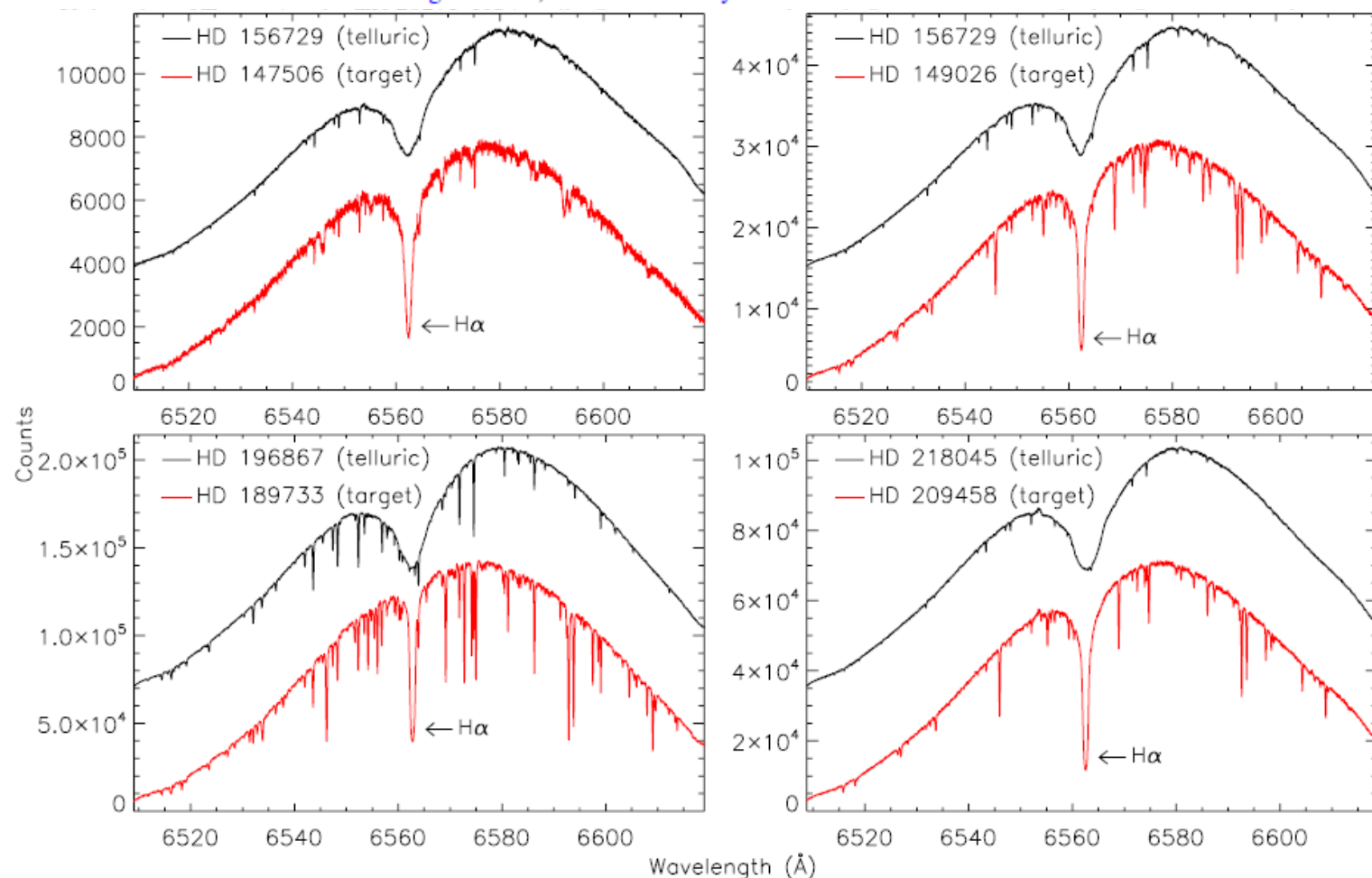
We concentrated our search for the  $J = 6_{16}-5_{23}$  transition of the water maser line ( $f = 22235.08 \text{ MHz}$ ) in two of the strongest H(II) regions in the LMC<sup>6</sup>—N157 (ref. 7, 30 Doradus) and N159—and in two dark nebulae<sup>8</sup>—Hodge 47 and Hodge 52. Huggins *et al.*<sup>9</sup> studied these four regions in their carbon monoxide survey.



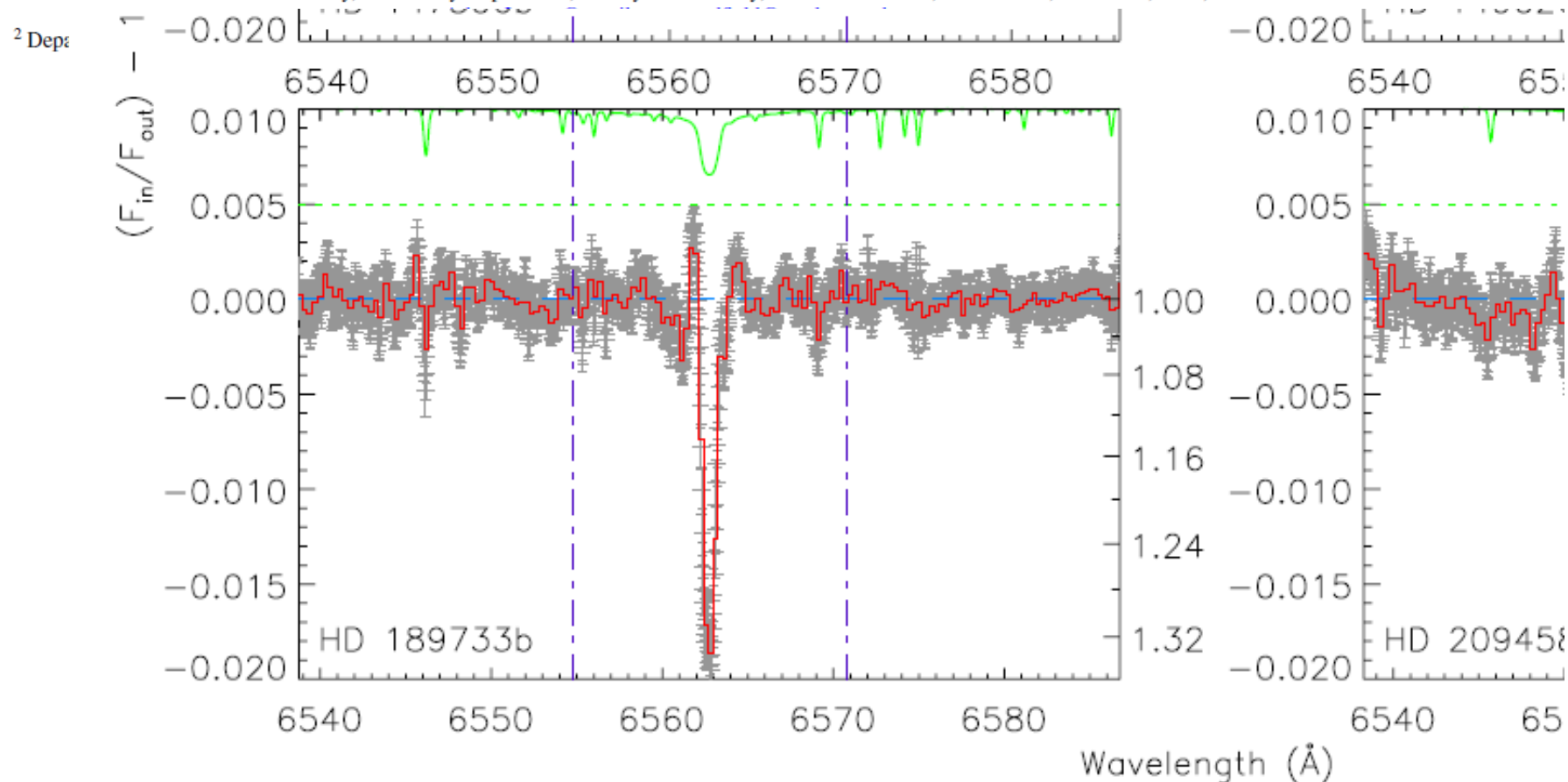
$$\Delta v = 1,35 \text{ km/s}$$

$$R = 221\ 000$$

**Fig. 1** Water vapour spectrum of N159 (RA 05 h 40 min 24 s DEC.  $-69^{\circ}46'.0, 1950.0$ ). The main feature appears at  $233.6 \text{ km s}^{-1}$  with respect to the Local Standard of Rest.

R  $\sim$  60 000, HRS (HET/McDonald) – single-objectA DETECTION OF H $\alpha$  IN AN EXOPLANETARY EXOSPHEREADAM G. JENSEN<sup>1</sup>, SETH REDFIELD<sup>1</sup>, MICHAEL ENDL<sup>2</sup>, WILLIAM D. COCHRAN<sup>2</sup>, LARS KOESTERKE<sup>2,3</sup>, AND TRAVIS BARMAN<sup>4</sup><sup>1</sup> Van Vleck Observatory, Astronomy Department, Wesleyan University, 96 Foss Hill Drive, Middletown, CT 06459, USA;[Adam.Jensen@gmail.com](mailto:Adam.Jensen@gmail.com), [sredfield@wesleyan.edu](mailto:sredfield@wesleyan.edu)<sup>2</sup> Department of Astr  
<sup>3</sup> Texas

**Figure 1.** Examples of the spectra in the echelle order that contains H I  $\lambda$ 6562 for all four targets, along with the spectra of their respective telluric standard stars from the same night of observation. All spectra are reduced from the raw echelle images but are not processed with the additional steps we discuss in Section 2.2 (including removal of the H $\alpha$  feature from the telluric spectra, telluric correction from the primary target, and normalization). The target spectra are shown on the count scale of the y-axis, but the telluric spectra are scaled to have the same maximum as the corresponding target spectra and then arbitrarily shifted by 25% of that same maximum. The global shapes of the spectra are dominated by the blaze function of the echelle.

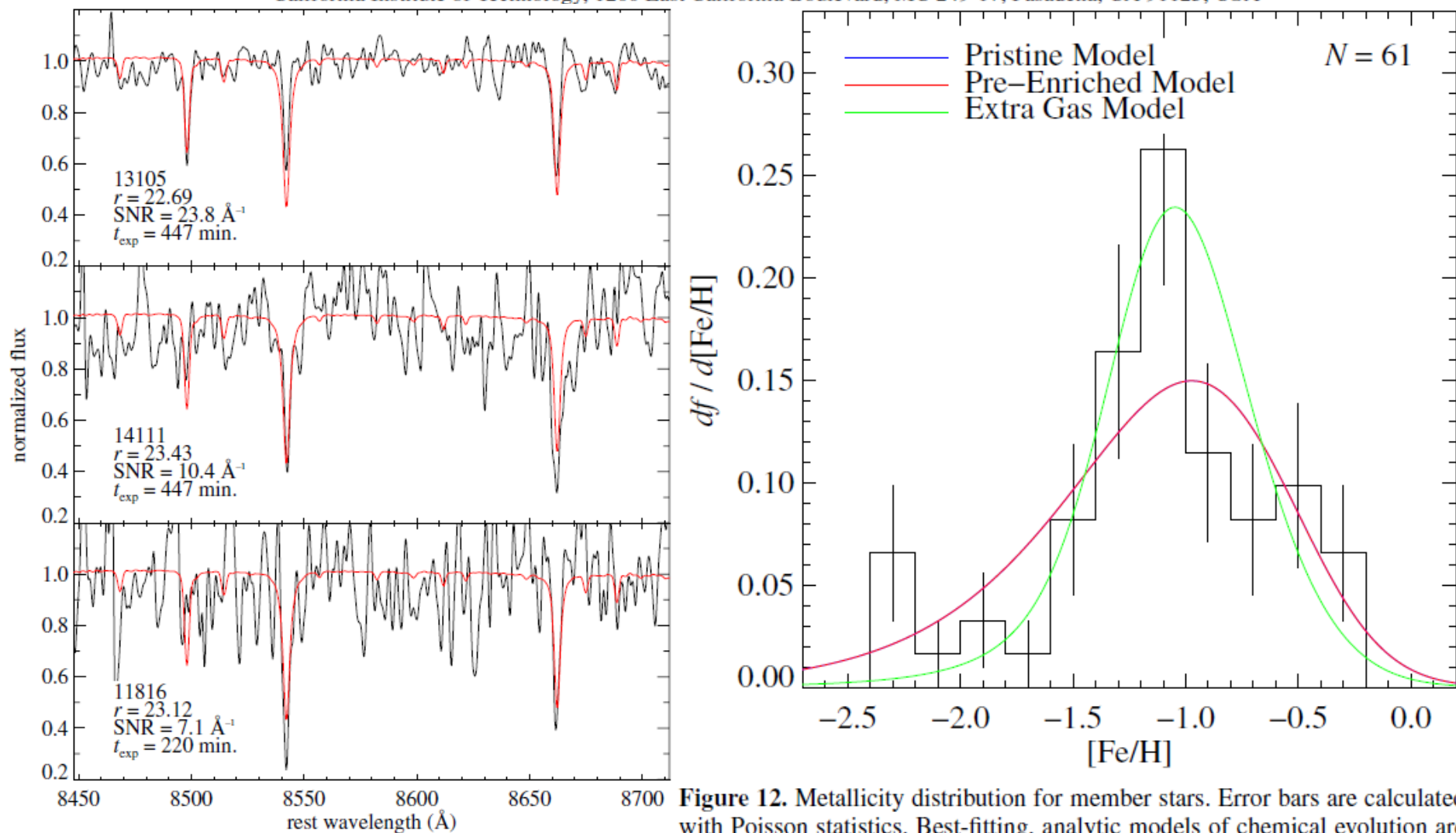
A DETECTION OF  $H\alpha$  IN AN EXOPLANETARY EXOSPHEREADAM G. JENSEN<sup>1</sup>, SETH REDFIELD<sup>1</sup>, MICHAEL ENDL<sup>2</sup>, WILLIAM D. COCHRAN<sup>2</sup>, LARS KOESTERKE<sup>2,3</sup>, AND TRAVIS BARMAN<sup>4</sup><sup>1</sup> Van Vleck Observatory, Astronomy Department, Wesleyan University, 96 Foss Hill Drive, Middletown, CT 06459, USA;

**Figure 3.** The  $H\alpha$  transmission spectra of our four targets. The binned transmission spectrum is shown in red (with error bars) and the unbinned transmission spectrum is shown in grey (with error bars). For reference, the master out-of-transit spectrum of the star is shown at the top with green line. The y-axis of the top plot is  $(F_{in}/F_{out}) - 1$ , showing the zero level and the top of each plot being unity in the normalized spectrum. A blue dashed line shows the central wavelength of the  $H\alpha$  line, and purple vertical dot-dashed lines define the bandpass that is integrated to make our absorption measurements; the x-axis of the top plot is Wavelength ( $\text{\AA}$ ) to the edges of the plot.

R  $\sim$  7000, DEIMOS (Keck) – multi-object

## THE DYNAMICS AND METALLICITY DISTRIBUTION OF THE DISTANT DWARF GALAXY VV124\*

1,1 Mpc

EVAN N. KIRBY<sup>1,3</sup>, JUDITH G. COHEN<sup>1</sup>, AND MICHELE BELLAZZINI<sup>2</sup><sup>1</sup> California Institute of Technology, 1200 East California Boulevard, MC 249-17, Pasadena, CA 91125, USA

**Figure 12.** Metallicity distribution for member stars. Error bars are calculated with Poisson statistics. Best-fitting, analytic models of chemical evolution are shown as colored curves. The red and blue lines overlap almost exactly.

The most metal-rich white dwarf:  
 a tidally disrupted asteroid  
 Dufour et al. 2010 ApJ 719,  
 803

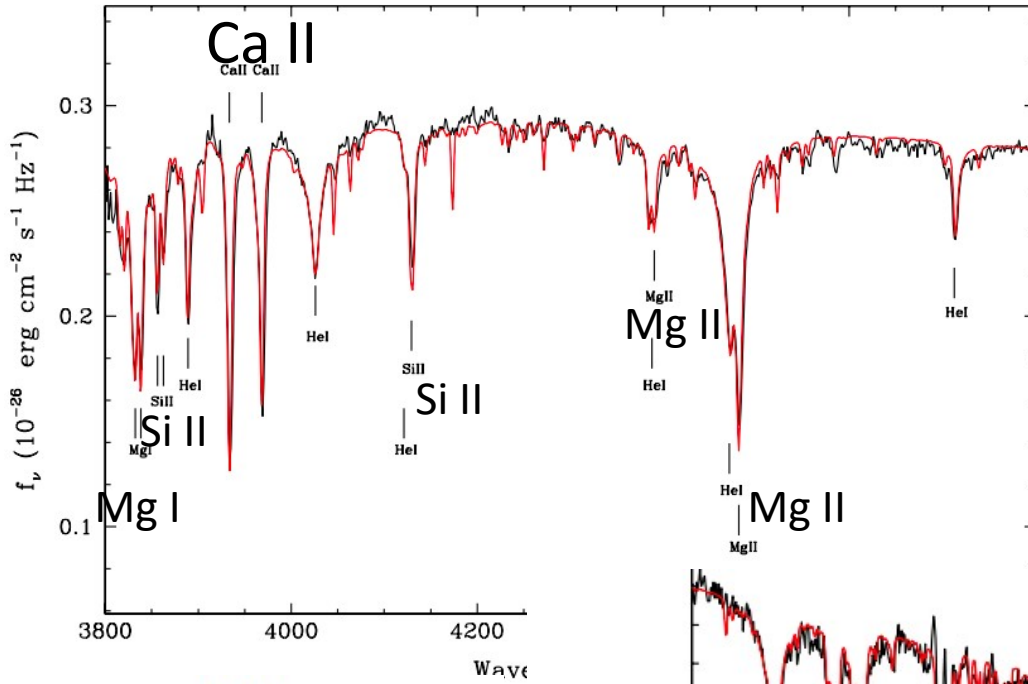
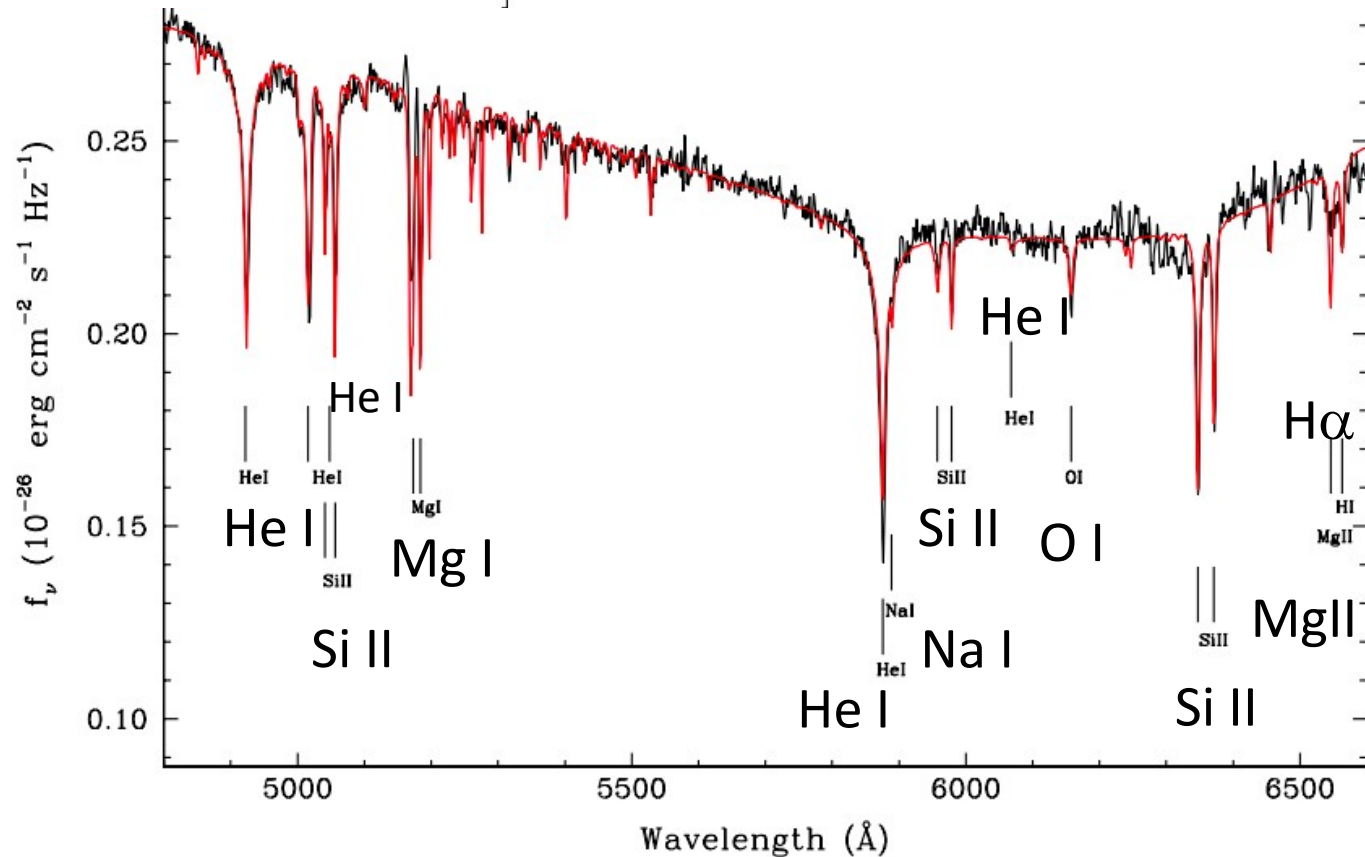


**Table 1**  
 Stellar Parameters for SDSS J0738+1835

Parameter	Value
$T_{\text{eff}}(\text{K})$	$13600 \pm 300$
$\log g$	$8.5 \pm 0.2$
$M_{\text{WD}}/M_{\odot}$	$0.907 \pm 0.128$
$M_{\text{init}}/M_{\odot}$	$4.4 \pm 1.0^{\text{a}}$
$R/R_{\odot}$	$0.00886 \pm 0.0015$
$\log L/L_{\odot}$	$-2.62 \pm 0.14$
$D$	$136 \text{ pc} \pm 22$
Cooling age	$595 \text{ Myr} \pm 219$
$\log \text{H}/\text{He}$	$-5.7 \pm 0.3$
$\log \text{O}/\text{He}$	$-4.0 \pm 0.2$
$\log \text{Mg}/\text{He}$	$-4.7 \pm 0.2$
$\log \text{Si}/\text{He}$	$-4.9 \pm 0.2$
$\log \text{Ca}/\text{He}$	$-6.8 \pm 0.3$
$\log \text{Fe}/\text{He}$	$-5.1 \pm 0.3$





White dwarfs with metals in the spectrum may be engulfing rocky material



# Chemical signatures of rocks in White Dwarfs

THE ASTROPHYSICAL JOURNAL, 584:L91–L94, 2003 February 20

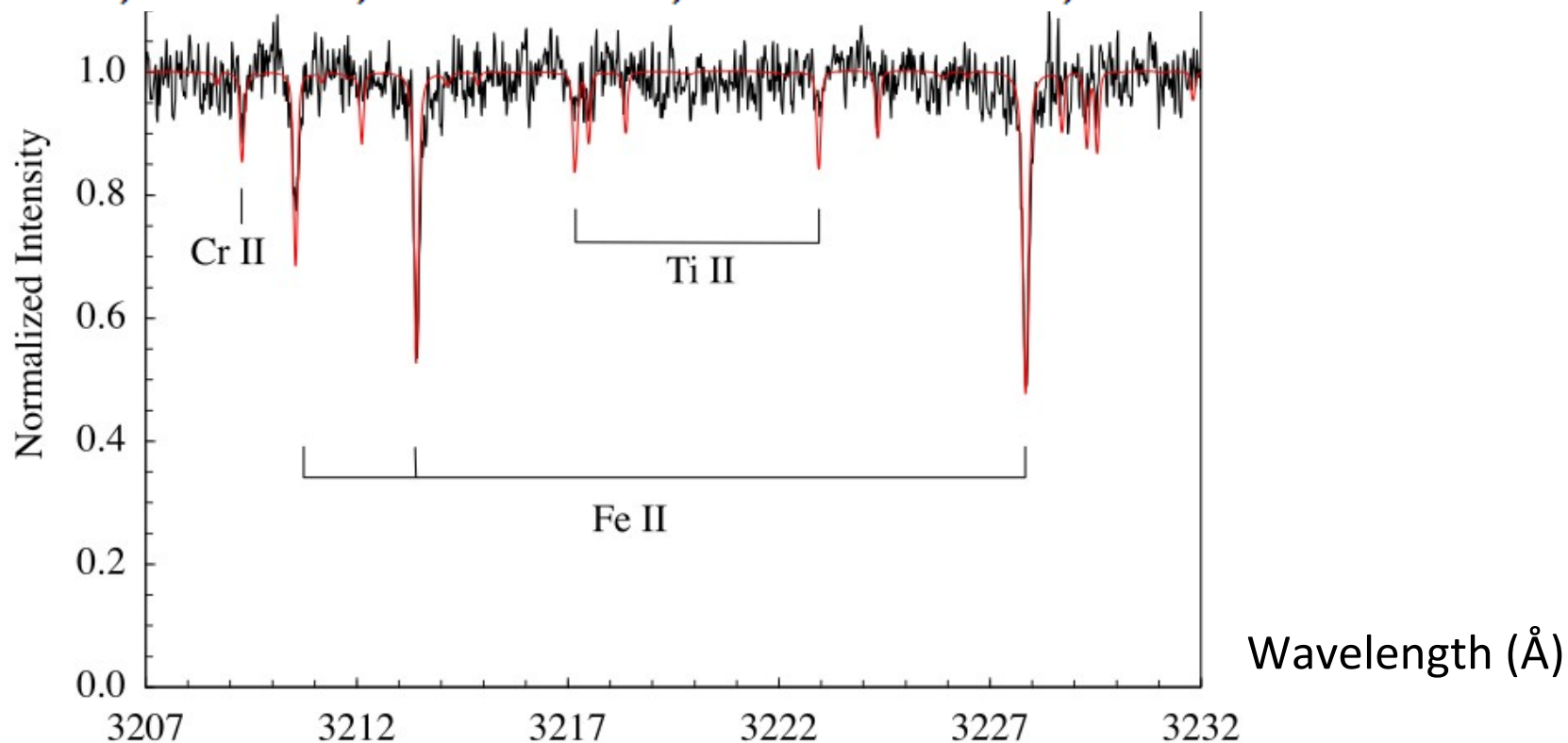
A TIDALLY DISRUPTED ASTEROID AROUND THE WHITE DWARF G29-38

M. JURA

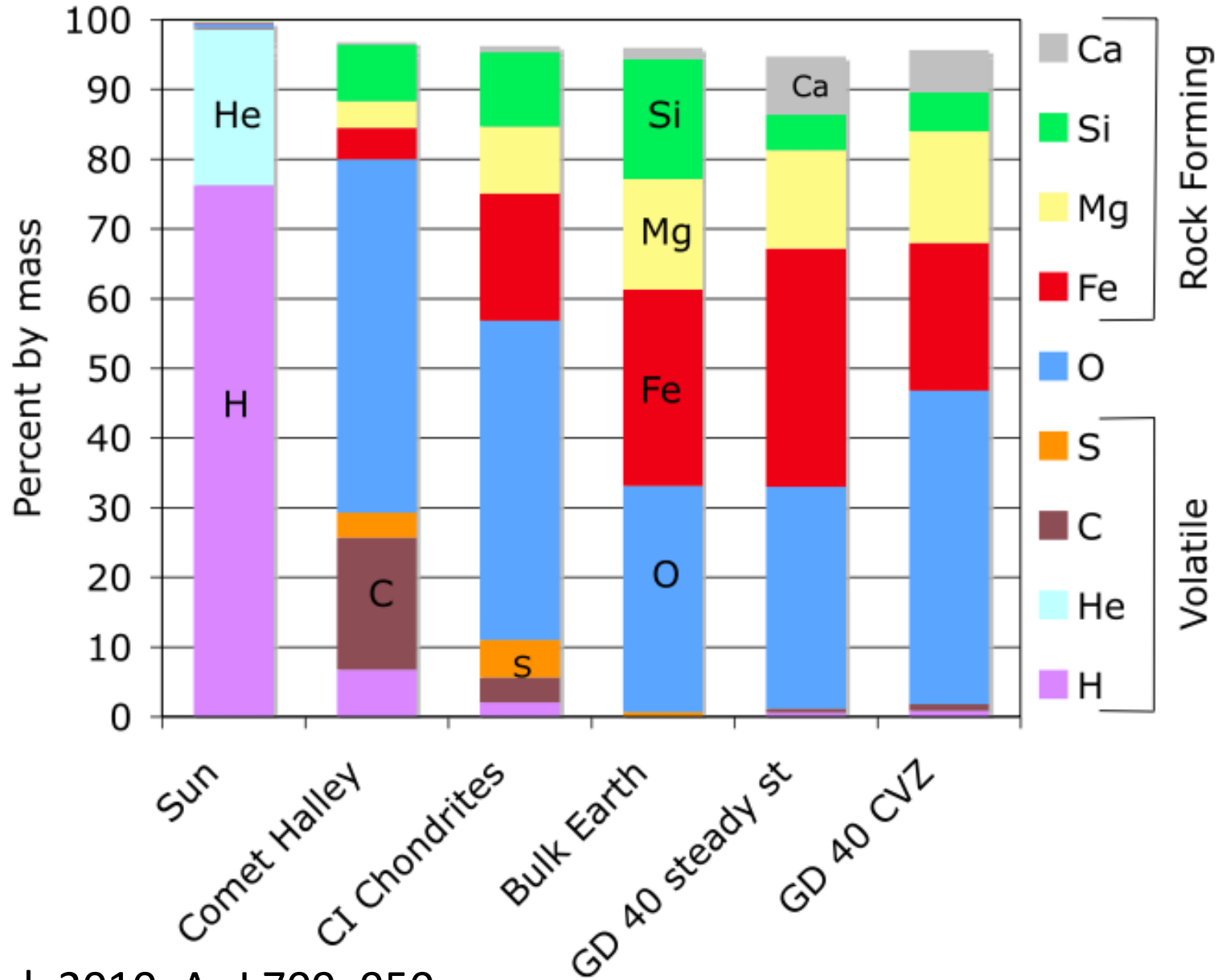
THE ASTROPHYSICAL JOURNAL, 709:950–962, 2010 February 1

CHEMICAL ABUNDANCES IN THE EXTERNALLY POLLUTED WHITE DWARF GD 40: EVIDENCE OF A ROCKY EXTRASOLAR MINOR PLANET

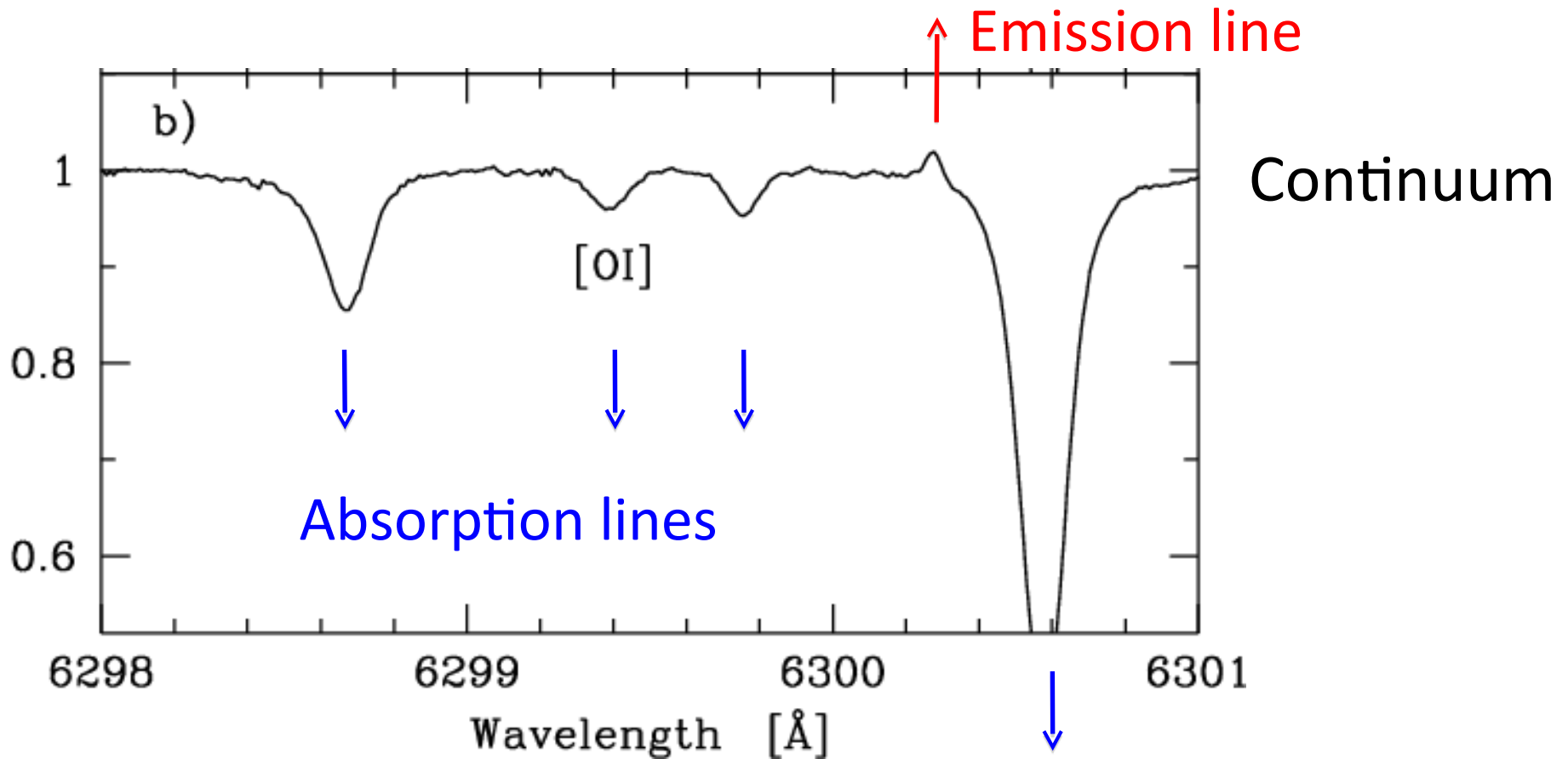
B. KLEIN<sup>1</sup>, M. JURA<sup>1</sup>, D. KOESTER<sup>2</sup>, B. ZUCKERMAN<sup>1</sup>, AND C. MELIS<sup>1,3</sup>



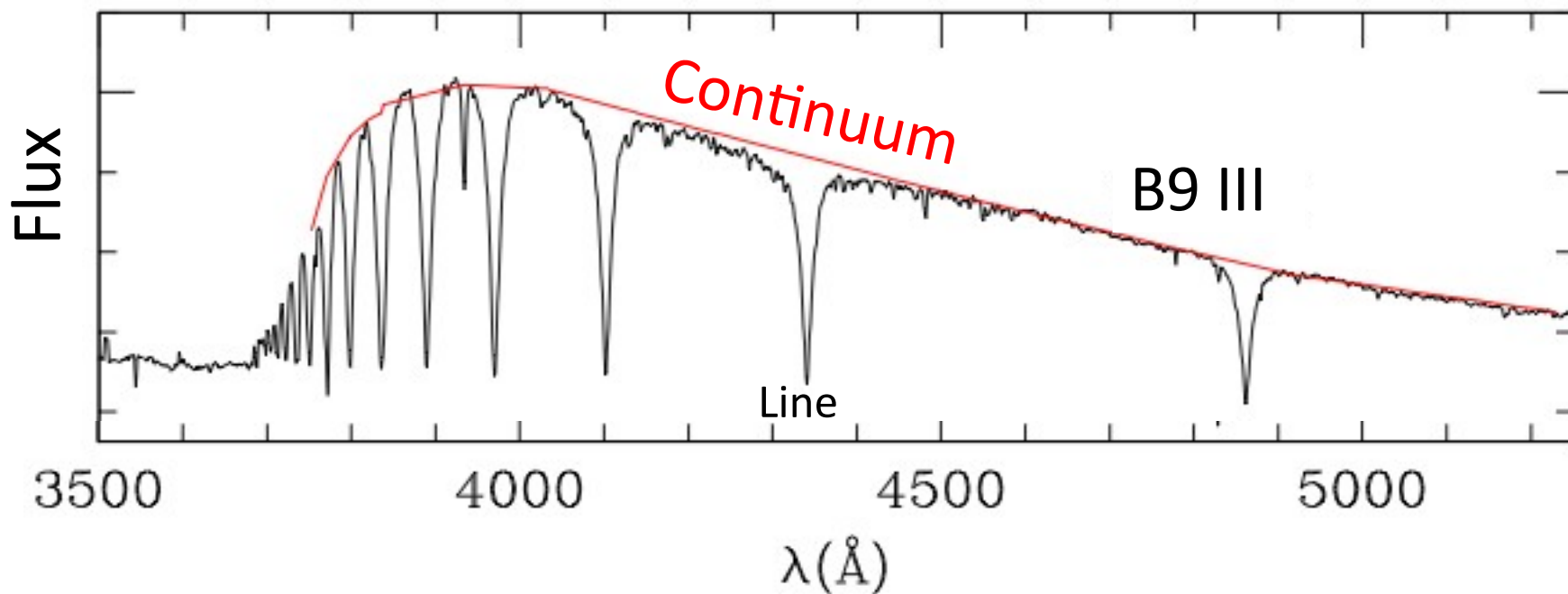
# Chemical signatures of rocky material in White Dwarfs



# Terminology for spectral lines



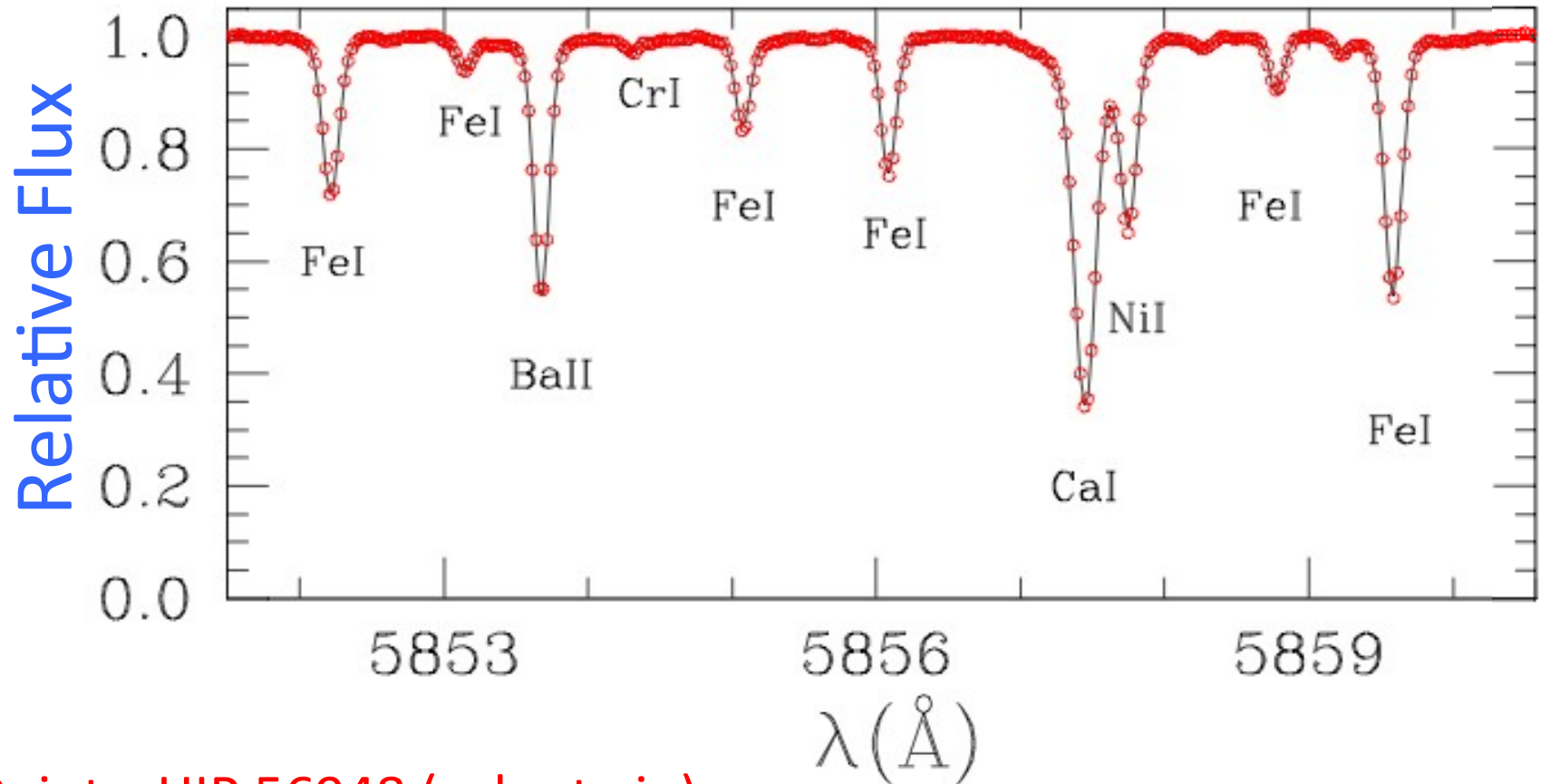
# Continuum: the region without line absorption



Absorption lines from the Balmer series in star B9 III ( $\sim$  A0 III)

# Normalized spectrum

Relative flux = flux / continuo

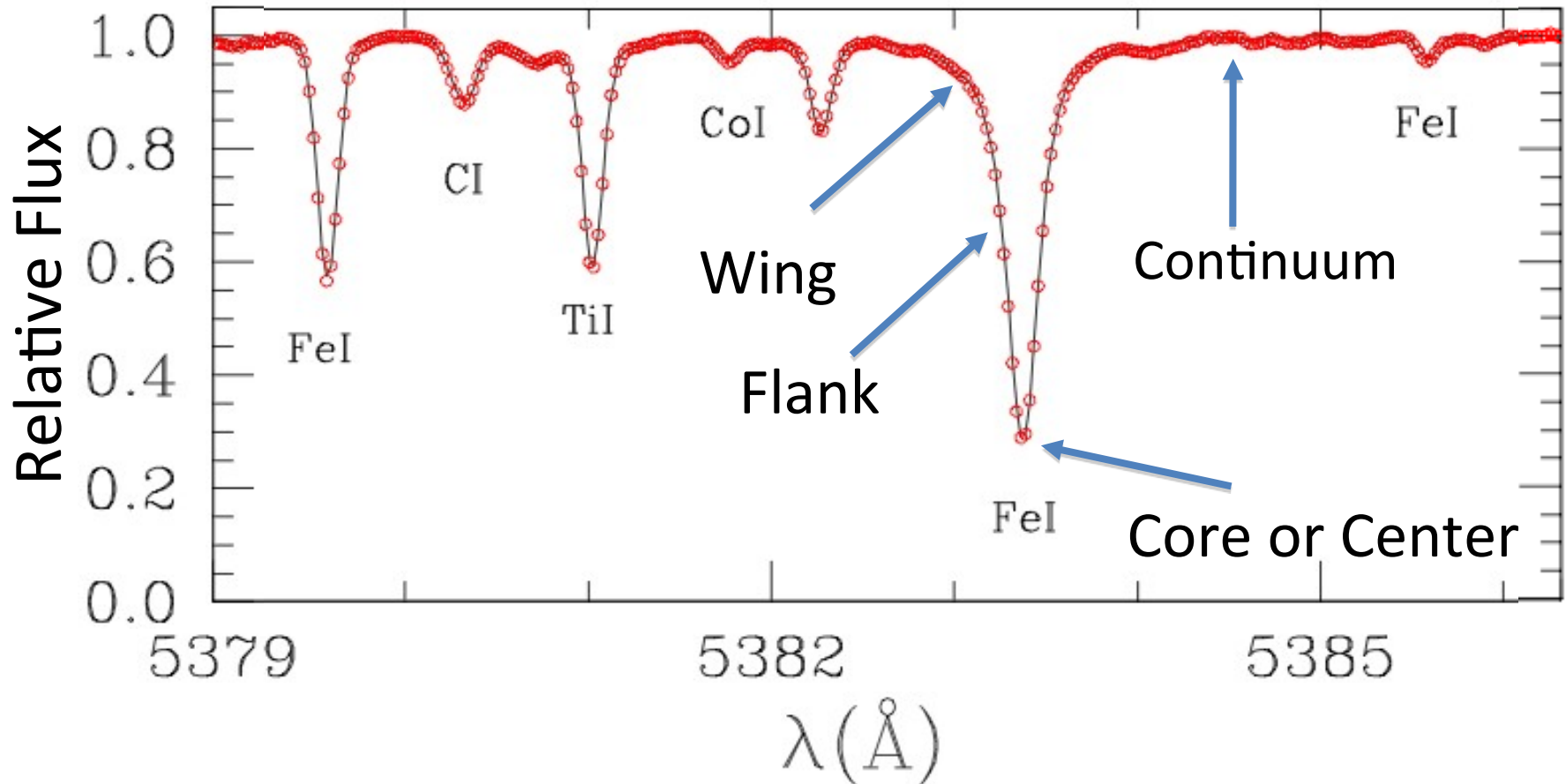


Points: HIP 56948 (solar twin)

Solid line: Sun

Meléndez et al. (2012, A&A 543, A29)

All lines show “wings”, but they are more clear in the stronger lines

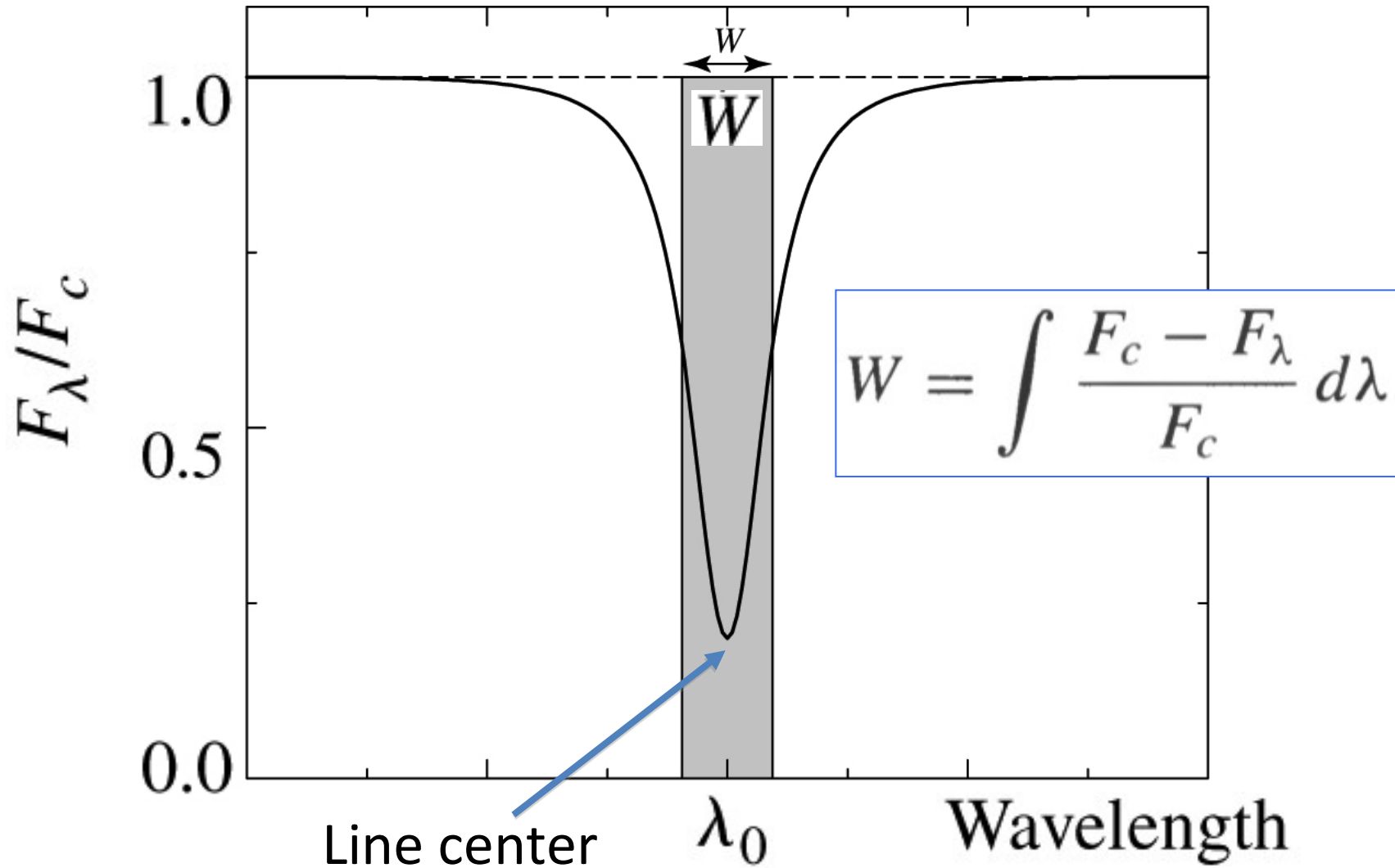


Points: HIP 56948 (solar twin)

Solid line: Sun

Meléndez et al. (2012, A&A 543, A29)

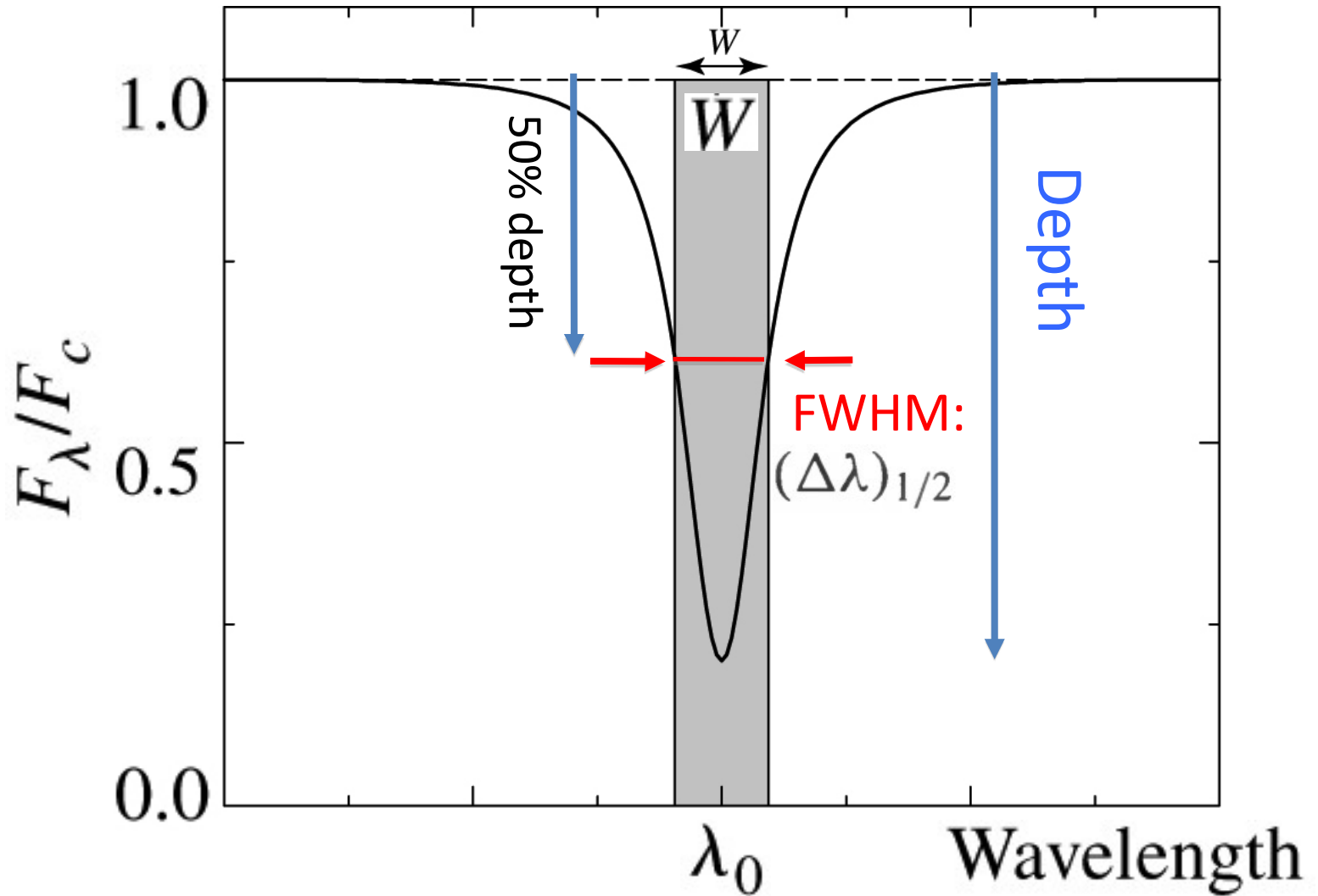
The strength of a line can be quantified by its **equivalent Width ( $W$ )**



In the optical, absorption lines  $W \sim 0.01$  nm. Weak lines,  $W \sim 10^{-3}$  nm.



# Line **Depth** and Full Width at Half Maximum (**FWHM**)



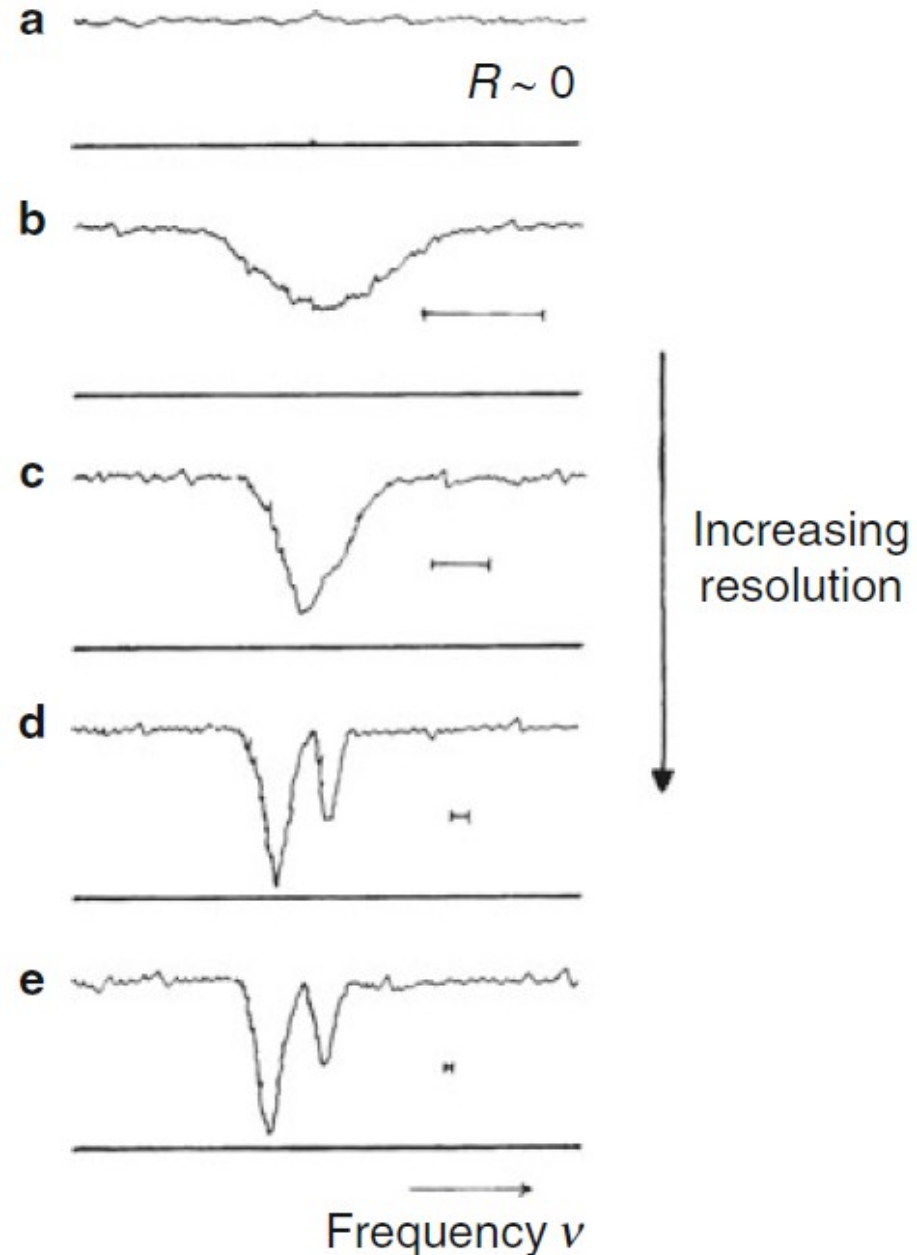
# Spectral resolution $\Delta\nu$

Resolving power  $R = \nu/\Delta\nu$

**Fig. 8.4** Observation of a spectral line at increasing resolution. (a)  $R \sim 0$ .

(b) The line appears. (c) The line appears double, but unresolved (*blended*). (d) The two lines are resolved.

(e) The true width of the lines is attained, and line purity can be no further improved by increasing  $R$ . The *horizontal line* shows the instrumental spectral width  $\Delta\nu = \nu_0/R$  used in each observation



# Examples of spectral lines

**Table 8.1** Examples of discrete transitions

Transition	Energy [eV]	Spectral Region	Example
Hyperfine structure	$10^{-5}$	Radiofrequencies	21 cm hydrogen line
Spin-orbit coupling	$10^{-5}$	Radiofrequencies	1667 MHz transitions of OH molecule
Molecular rotation	$10^{-2}$ – $10^{-4}$	Millimetre and infrared	1–0 transition of CO molecule at 2.6 mm
Molecular rotation–vibration	$1$ – $10^{-1}$	Infrared	H <sub>2</sub> lines near 2 μm
Atomic fine structure	$1$ – $10^{-3}$	Infrared	Ne II line at 12.8 μm
Electronic transitions of atoms, molecules and ions	$10^{-2}$ – $10$	Ultraviolet, visible, infrared	Lyman, Balmer series, etc., of H, resonance lines of C I, He I, and K, L shell electron lines (Fe XV, O VI)
Nuclear transitions	$> 10^4$	X and γ rays	<sup>12</sup> C line at 15.11 keV
Annihilations	$\gtrsim 10^4$	γ rays	Positronium line at 511 keV

© Lena 3<sup>rd</sup> Ed or Table 5.1 2<sup>nd</sup> Ed.

# Spectral lines carry important information

## Characteristics

## Information

- |                   |  |
|-------------------|--|
| Line center:      | <ul style="list-style-type: none"><li>- Element, line transition</li><li>- Radial velocity (kinematics, binarity, planets)</li></ul> |
| Equivalent Width: | <ul style="list-style-type: none"><li>- Chemical composition</li><li>- Temperature, Gravity</li></ul>                                |
| FWHM:             | <ul style="list-style-type: none"><li>- Projected rotation velocity (<math>v \times \sin i</math>)</li></ul>                         |
| Profile:          | <ul style="list-style-type: none"><li>- Velocity field</li></ul>   |
| Flux variations:  | <ul style="list-style-type: none"><li>- H &amp; K lines (rotation, activity cycle)</li></ul>   |
| Polarization:     | <ul style="list-style-type: none"><li>- Magnetic field</li></ul>   |

# Convection

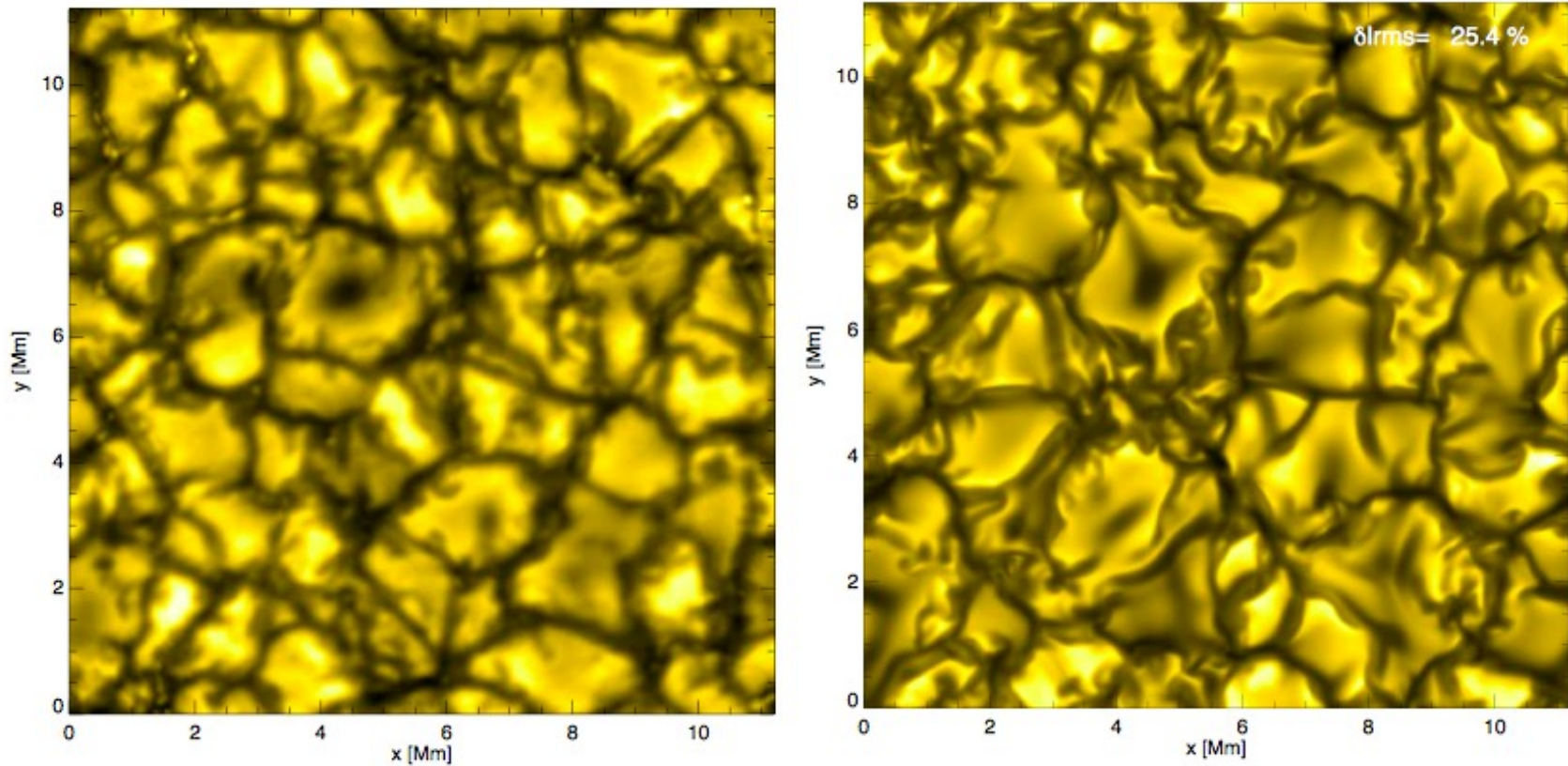
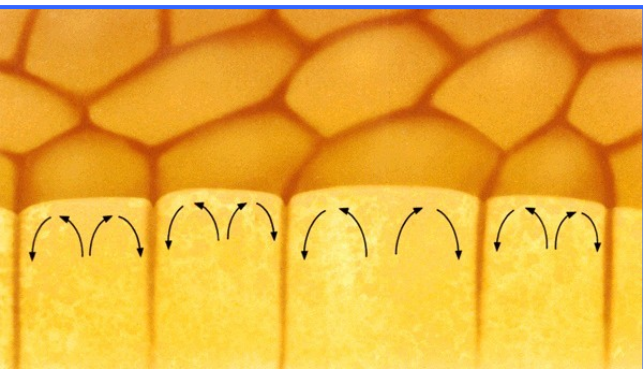
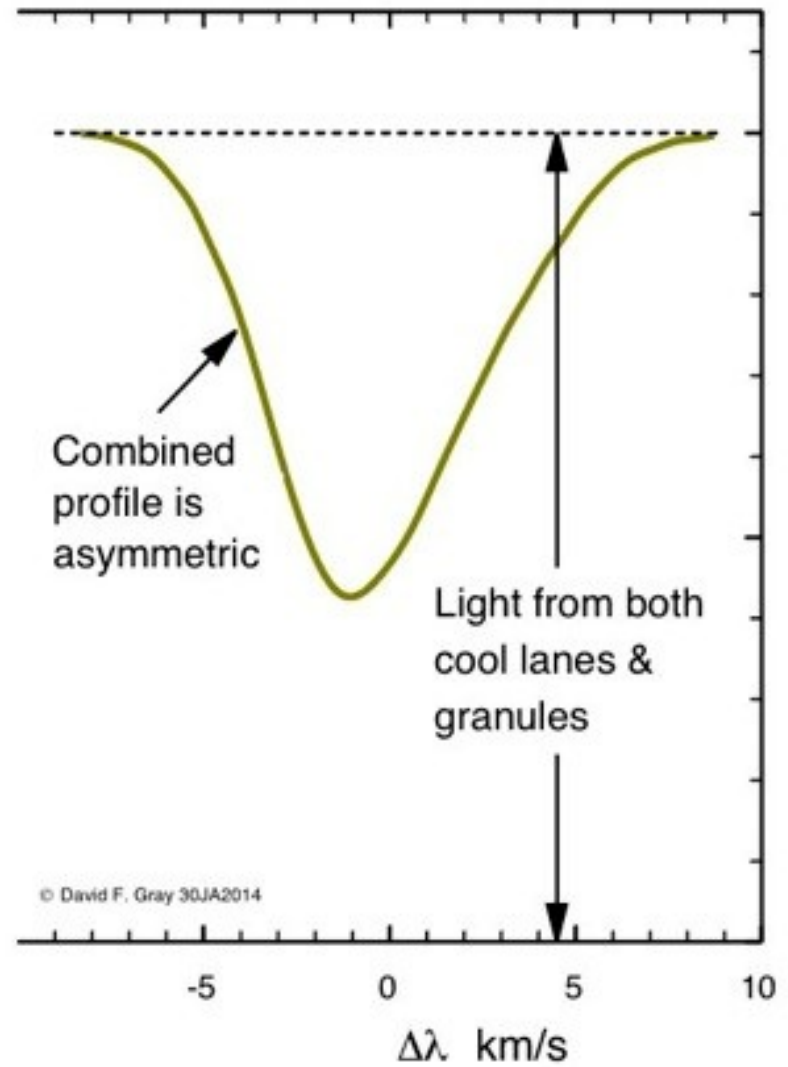
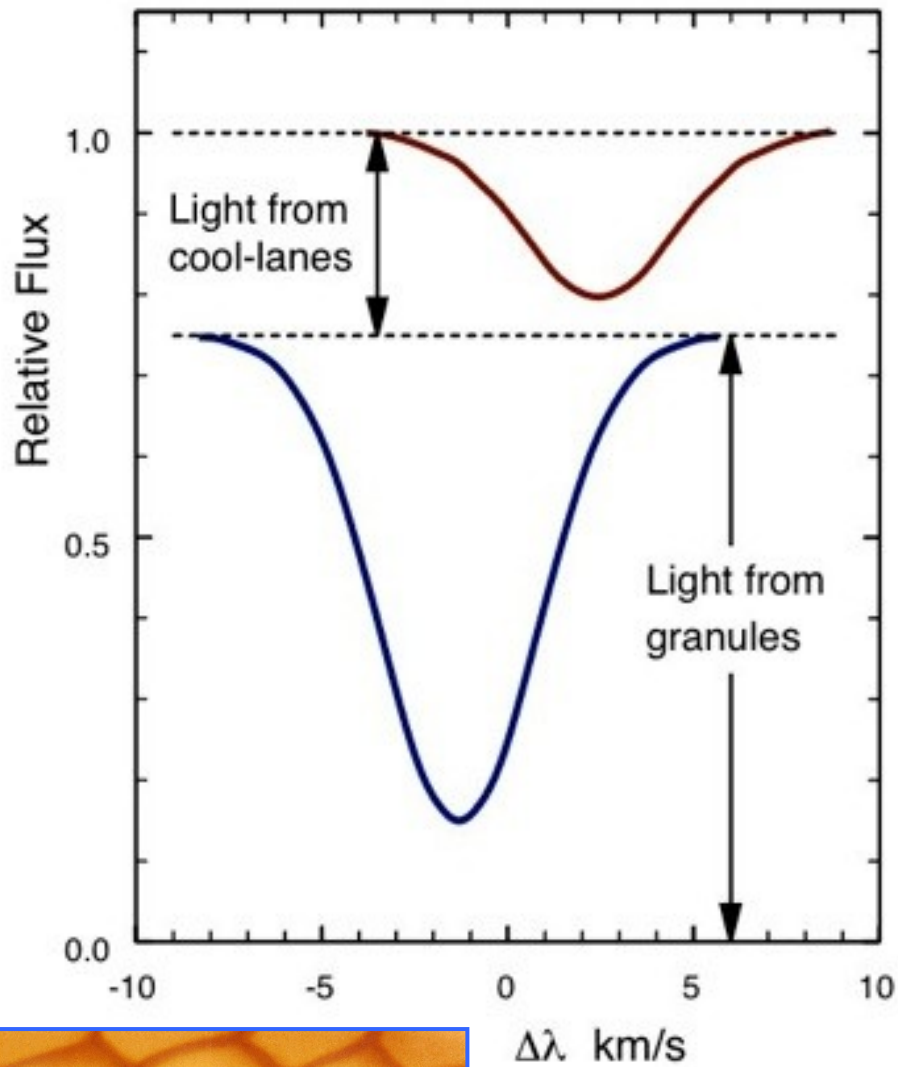


Figure 1: **Left:** Quiet solar granulation as observed with the 1m Swedish Solar Telescope (courtesy Mats Carlsson 2004). **Right:** High-resolution CO<sup>5</sup>BOLD simulation of solar surface convection. Both images show the emergent continuum intensity (using identical scaling) at  $\lambda 4364 \text{ \AA}$  in a field measuring  $15'' \times 15''$  ( $11 \times 11 \text{ Mm}$ ).

## **The Solar Photospheric Nitrogen Abundance. Determination with 3D and 1D model atmospheres.**

*E.Maiorca<sup>A</sup>, E.Caffau<sup>B</sup>, P.Bonifacio<sup>C,B,D</sup>, M.Busso<sup>A,H</sup>, R.Faraggiana<sup>E</sup>,  
M.Steffen<sup>F</sup>, H.-G.Ludwig<sup>C,B</sup>, I.Kamp<sup>G</sup>*

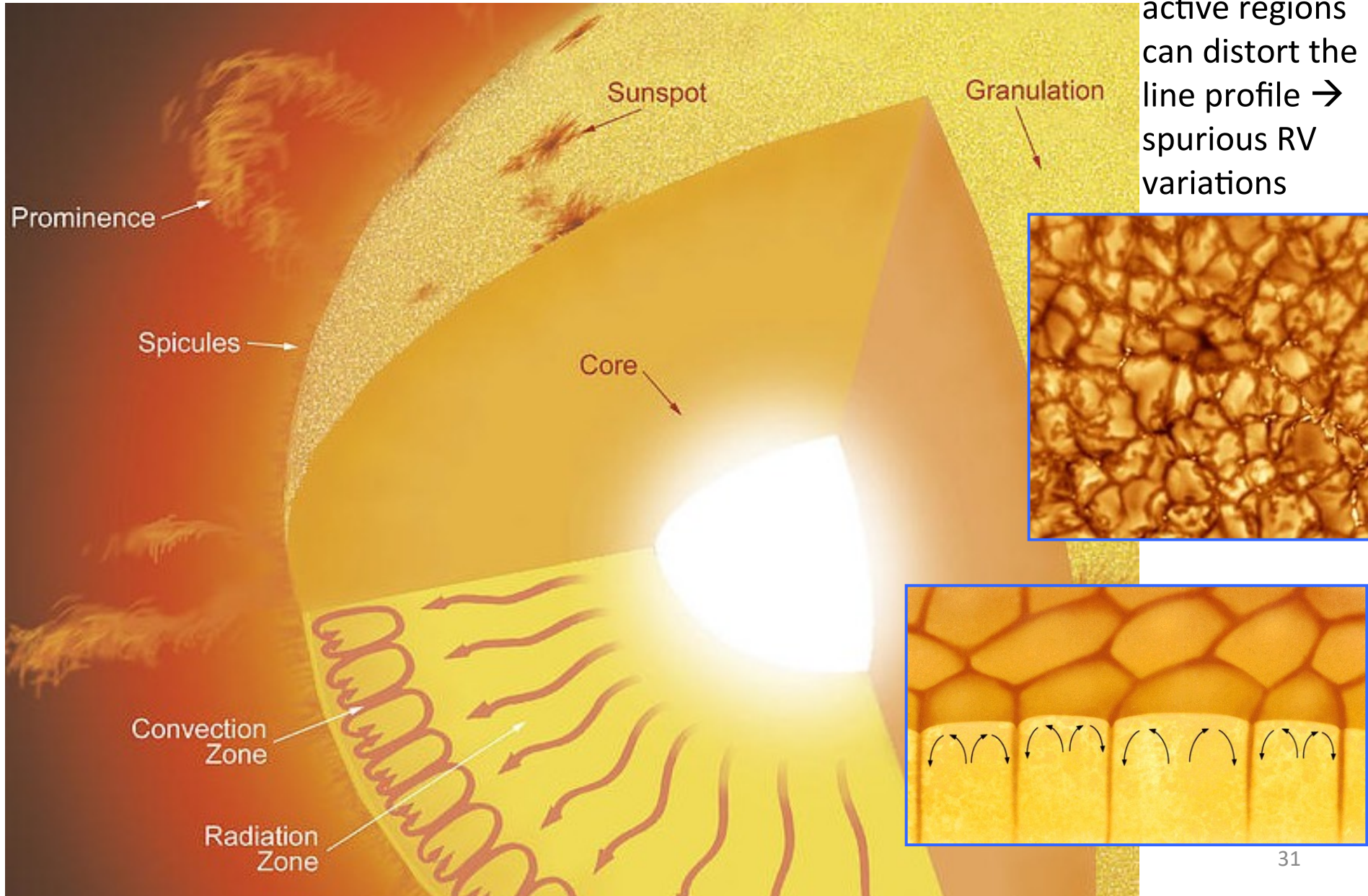


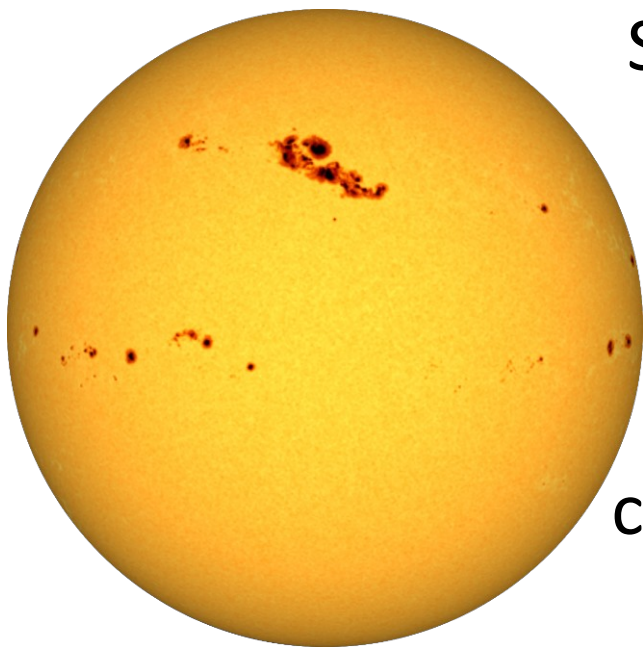
<http://astro.uwo.ca/~dfgray/Granulation.html>

Asymmetry in the line profile introduced by convection

# How to detect planets in an active star?

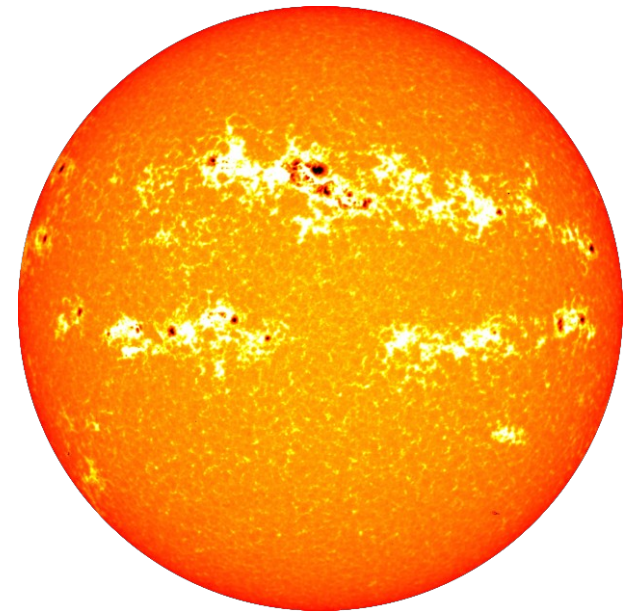
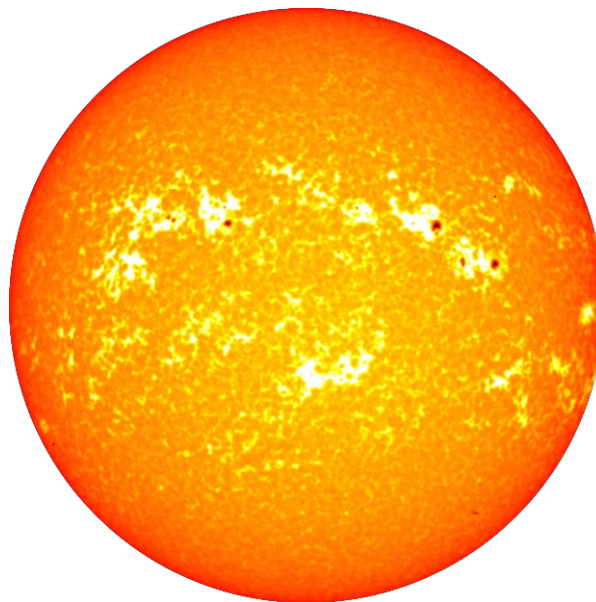
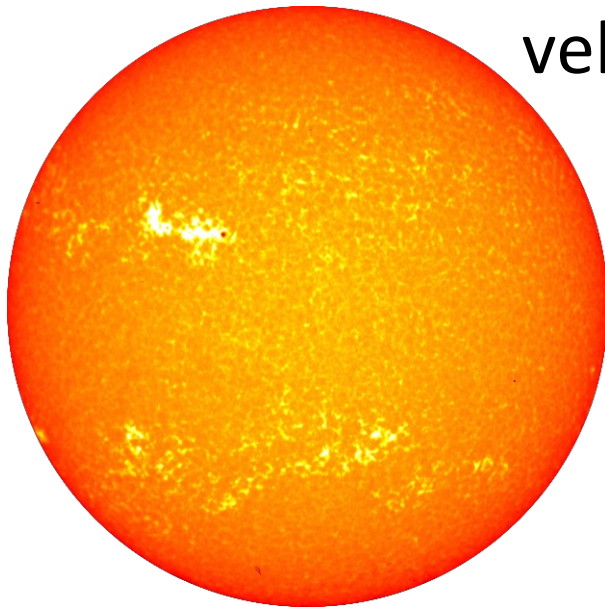
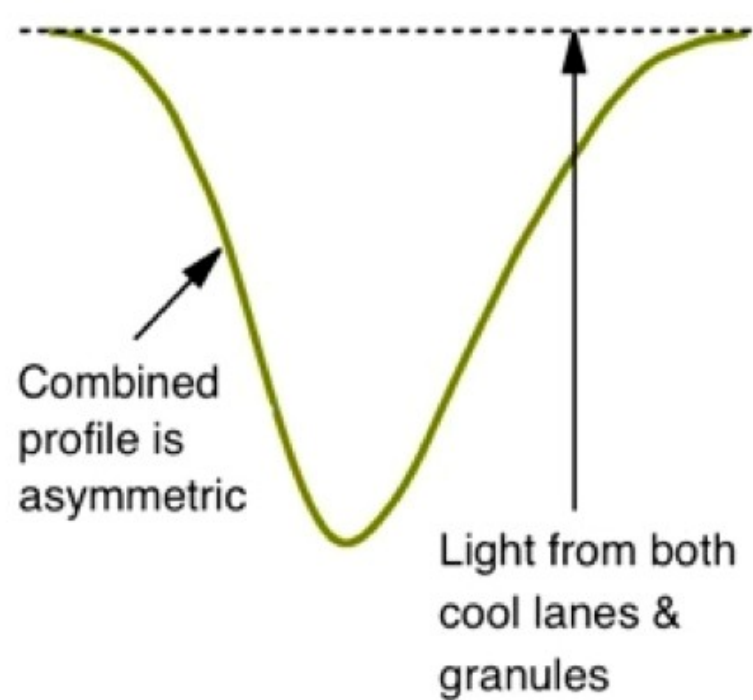
Suppression of convection in active regions can distort the line profile  $\rightarrow$  spurious RV variations





Suppression of convection in sunspots (left) and *plages* (*below*) can change the line profile

→ spurious radial velocity variations





# Basic components of the Spectrograph

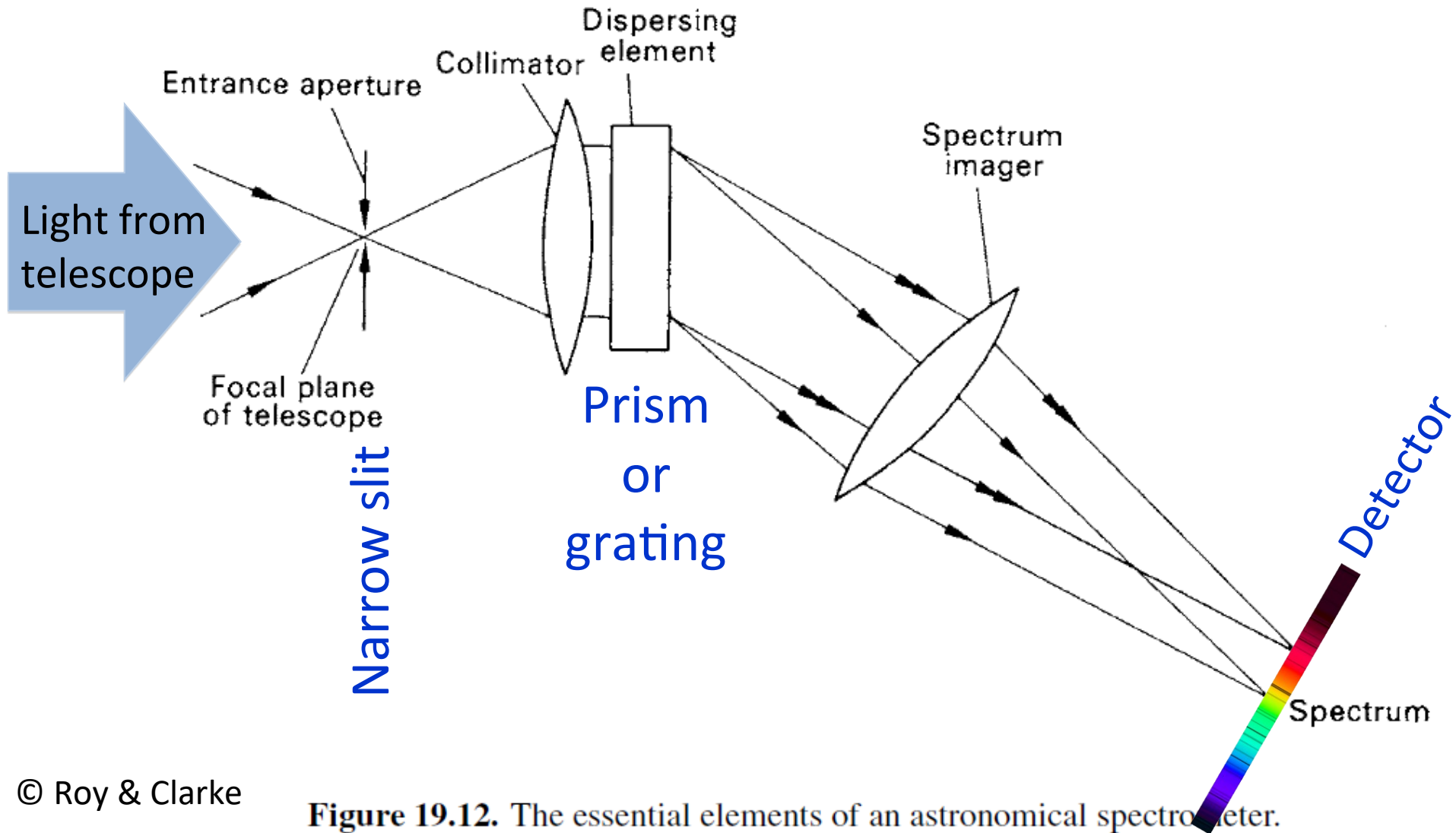
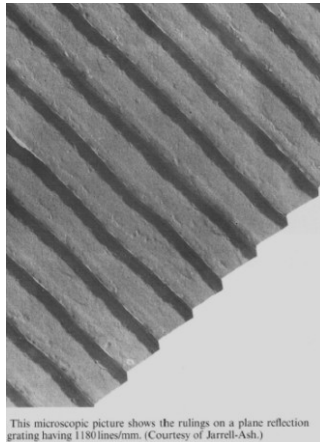


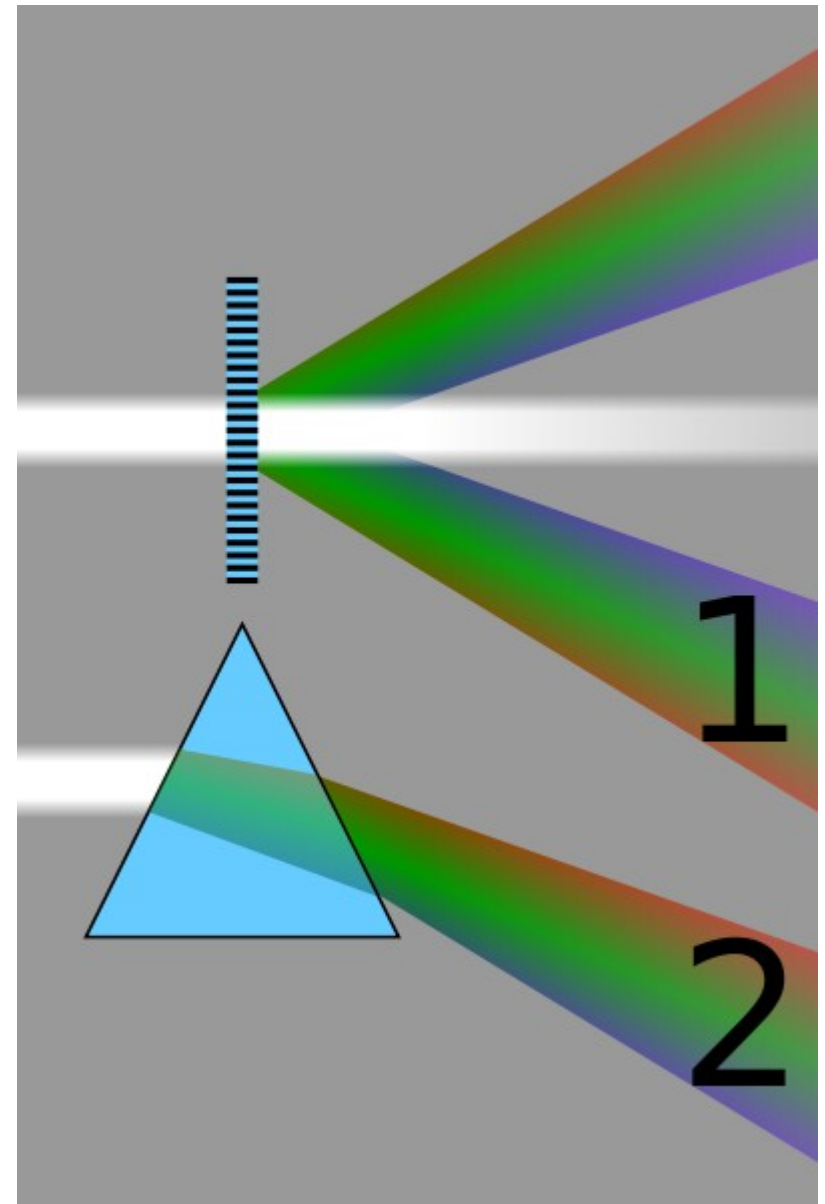
Figure 19.12. The essential elements of an astronomical spectrograph.

# Dispersing element

- Diffraction Grating: diffraction+interference



- Prism: differential refraction



# Prism as a dispersing element

$\theta_{\text{exit}} ?$

$$n_{\text{air}} \sin \theta_{\text{air}} = n_{\text{glass}} \sin \theta_{\text{glass}}$$

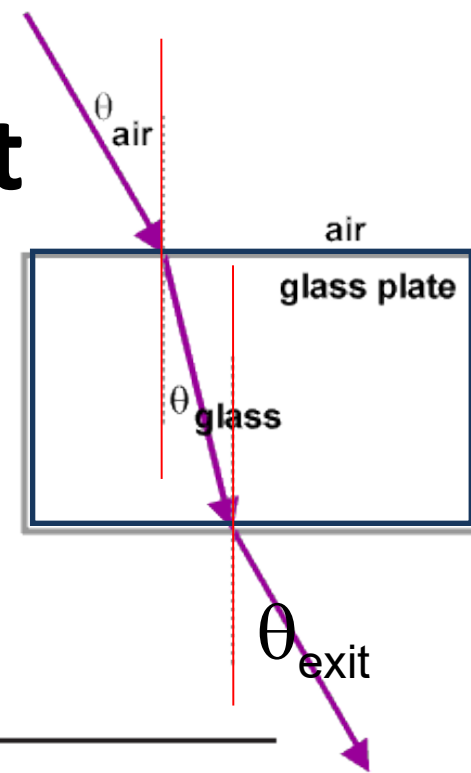


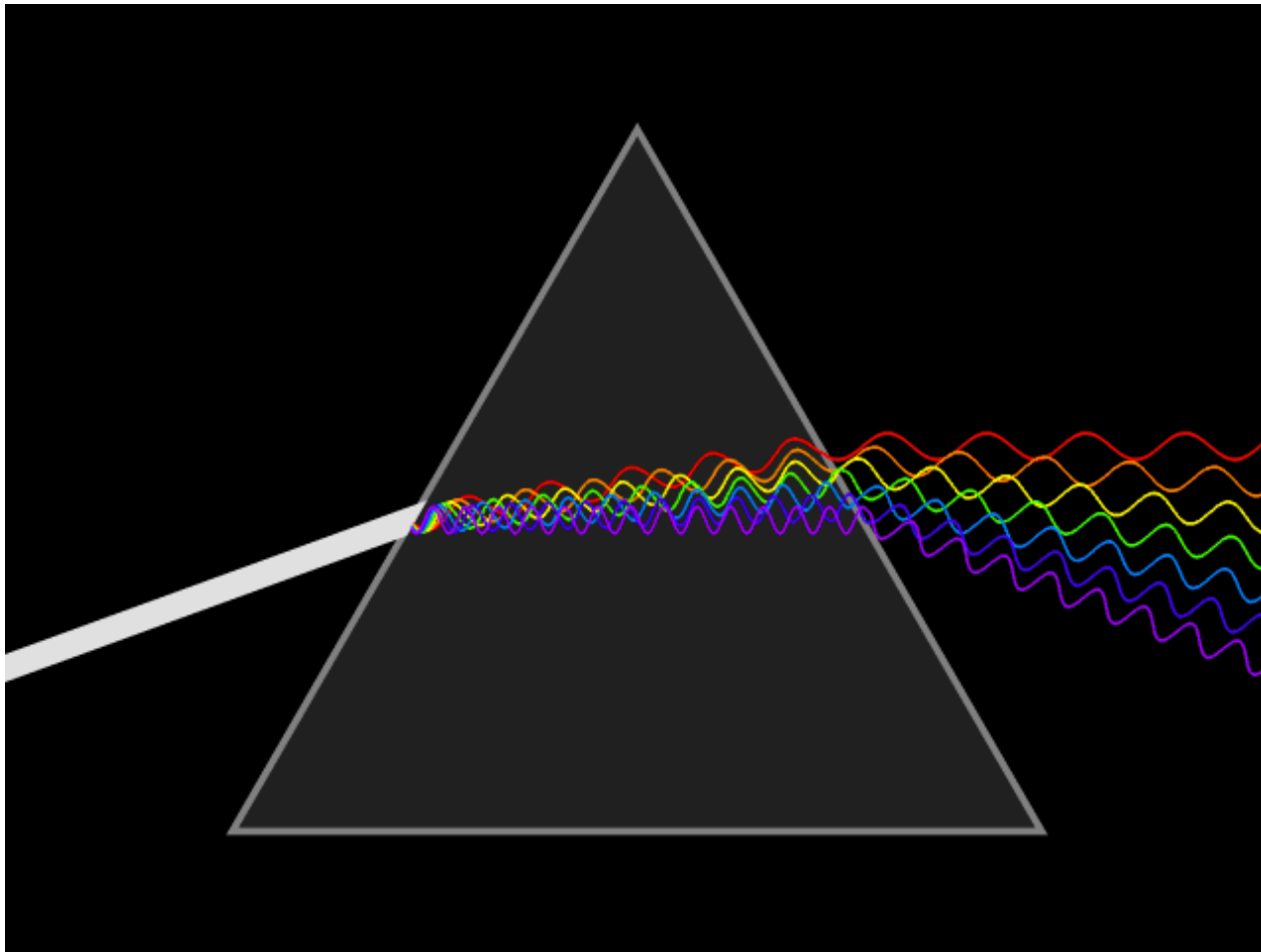
Table 1.1.5.

Refractive index at the specified wavelengths (nm)

Glass type	361	486	589	656	768
Crown	1.539	1.523	1.517	1.514	1.511
High dispersion crown	1.546	1.527	1.520	1.517	1.514
Light flint	1.614	1.585	1.575	1.571	1.567
Dense flint	1.705	1.664	1.650	1.644	1.638

$$n(\text{air}) = 1.0003$$

# Dispersing element: prism



# Snell law in a prism

$$\mu_1 \sin i = \mu_2 \sin r \quad (4.1.40)$$

$\mu_1$  (or  $n_1$ ) is  $\sim 1$  (air), so :  $n_1 \sin i_1 = n_2 \sin r_1$  means that  $n_2 = \sin i_1 / \sin r_1$

In the same way :  $n_2 \sin i_2 = n_1 \sin r_2 \rightarrow n_2 = \sin r_2 / \sin i_2$

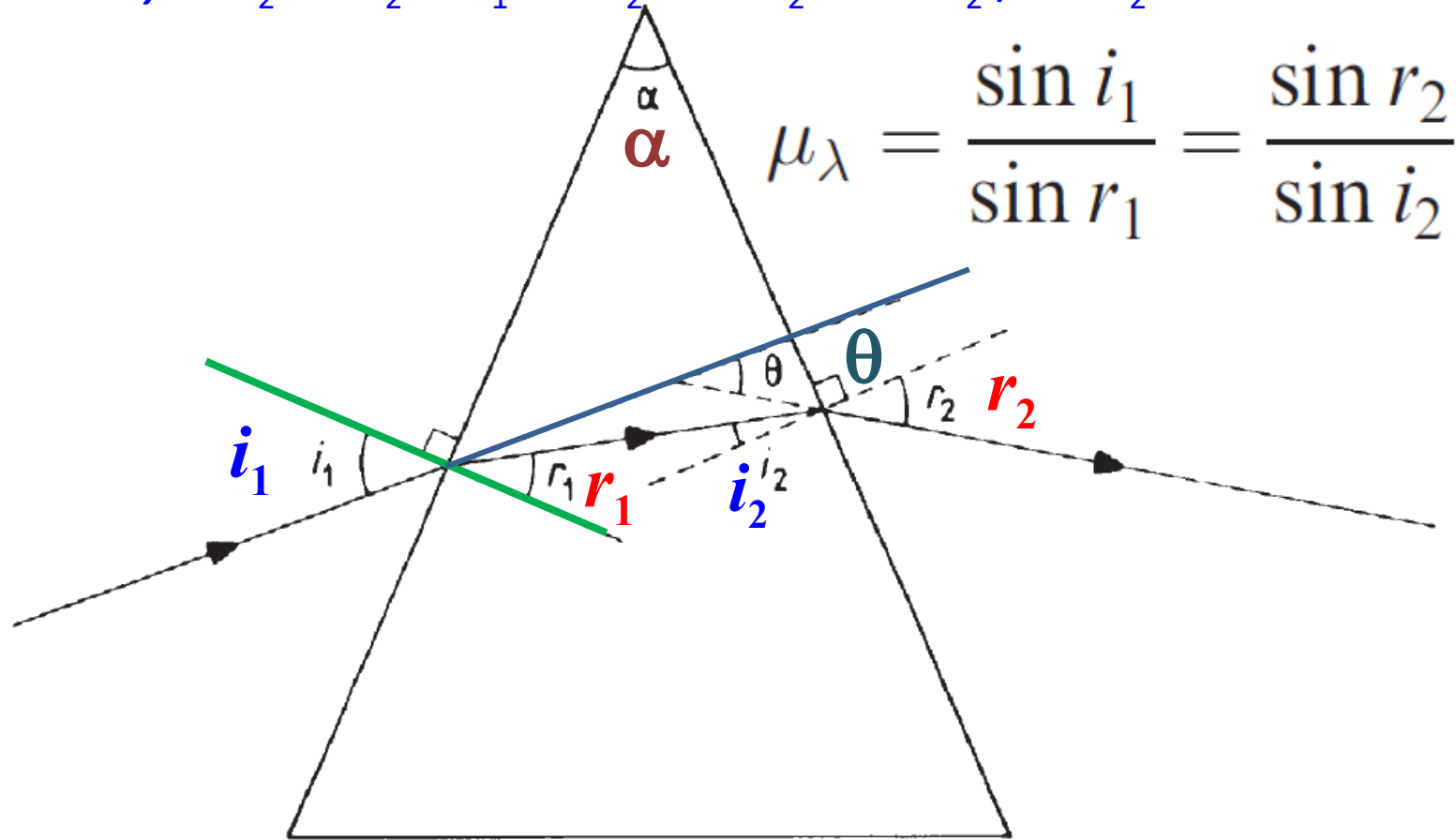


Figure 4.1.8. Optical path in a prism.

# Refractive index ( $\mu_\lambda$ or $n_\lambda$ ) varies with wavelength

In the visible the variation of  $n_\lambda$  may be approximated by the Hartmann dispersion formula.  $A$ ,  $B$  and  $C$  are known as the Hartmann constants

$$\mu_\lambda = A + \frac{B}{\lambda - C}. \quad (4.1.42)$$

**Table 1.1.5.**

Glass type	Refractive index at the specified wavelengths (nm)				
	361	486	589	656	768
Crown	1.539	1.523	1.517	1.514	1.511
High dispersion crown	1.546	1.527	1.520	1.517	1.514
Light flint	1.614	1.585	1.575	1.571	1.567
Dense flint	1.705	1.664	1.650	1.644	1.638

$$\mu_\lambda = A + \frac{B}{\lambda - C}. \quad (4.1.42)$$

If the refractive index is known at three different wavelengths, then we can obtain three simultaneous equations for the constants, from equation (4.1.42), giving

$$C = \frac{\left[ \left( \frac{\mu_1 - \mu_2}{\mu_2 - \mu_3} \right) \lambda_1 (\lambda_2 - \lambda_3) - \lambda_3 (\lambda_1 - \lambda_2) \right]}{\left[ \left( \frac{\mu_1 - \mu_2}{\mu_2 - \mu_3} \right) (\lambda_2 - \lambda_3) - (\lambda_2 - \lambda_3) \right]} \quad (4.1.43)$$

$$B = \frac{\mu_1 - \mu_2}{\left( \frac{1}{\lambda_1 - C} - \frac{1}{\lambda_2 - C} \right)} \quad (4.1.44)$$

$$A = \mu_1 - \frac{B}{\lambda_1 - C}. \quad (4.1.45)$$

The values for the constants for the optical region for typical optical glasses are:

	$A$	$B$	$C$
Crown glass	1.477	$3.2 \times 10^{-8}$	$-2.1 \times 10^{-7}$
Dense flint glass	1.603	$2.08 \times 10^{-8}$	$1.43 \times 10^{-7}$

$$\mu_\lambda = A + \frac{B}{\lambda - C}$$

Prisms uses apex  $\alpha = 60^\circ$

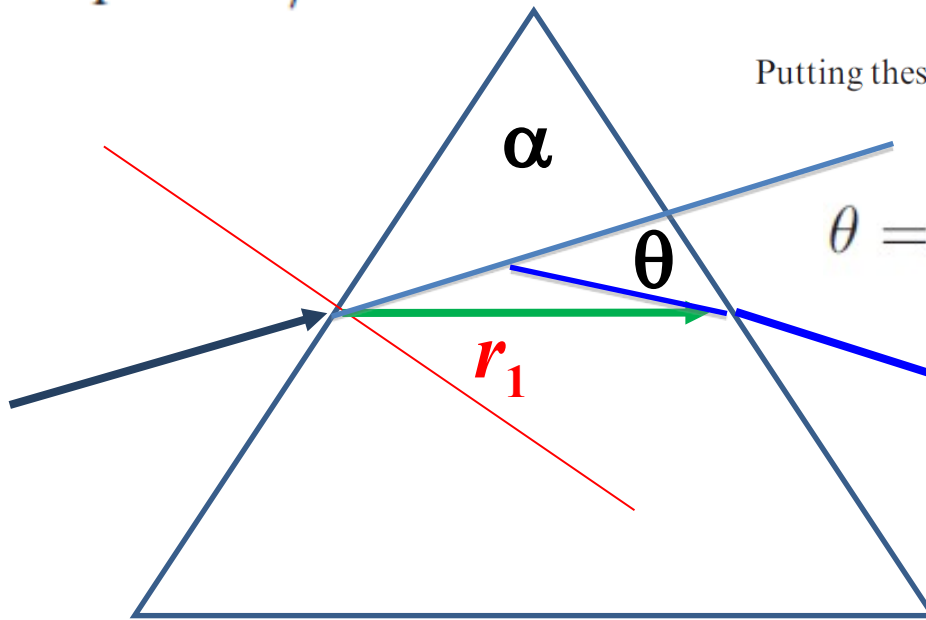
$$\theta = \sin^{-1}(\mu_\lambda \sin r_1) + \sin^{-1}[\mu_\lambda \sin(\alpha - r_1)] - \alpha$$

$$r_1 = \alpha/2$$

$$1.39 \times 10' \text{ }^\circ \text{ m}^{-1}$$

dispersion incidence of  $55.9^\circ$

Putting these values into equation (4.1.55) and using equation (4.1.42), we get



$$\theta = 2 \sin^{-1} \left\{ \frac{1}{2} \left[ A + \frac{B}{\lambda - C} \right] \right\} - 60$$

$$\frac{d\theta}{d\lambda} \approx \frac{-180AB}{\pi(\lambda - C)^2} \text{ }^\circ \text{ m}^{-1}$$

**dispersion of a prism increases rapidly towards shorter  $\lambda$**

(4.1.55)



# Spectrograph based on prism

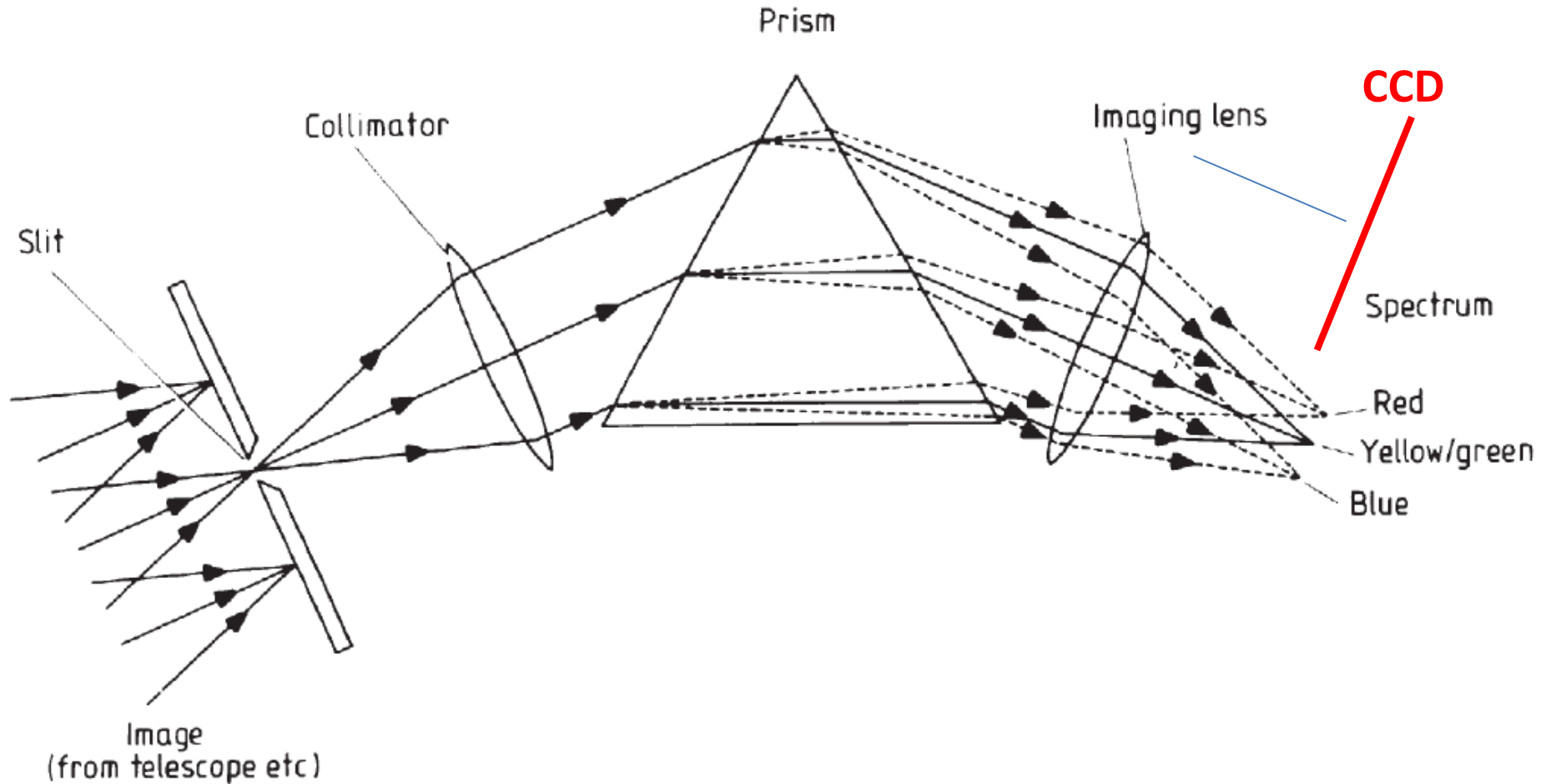


Figure 4.1.12. Basic optical arrangement of a prism spectroscope.

# Objective prism spectrograph

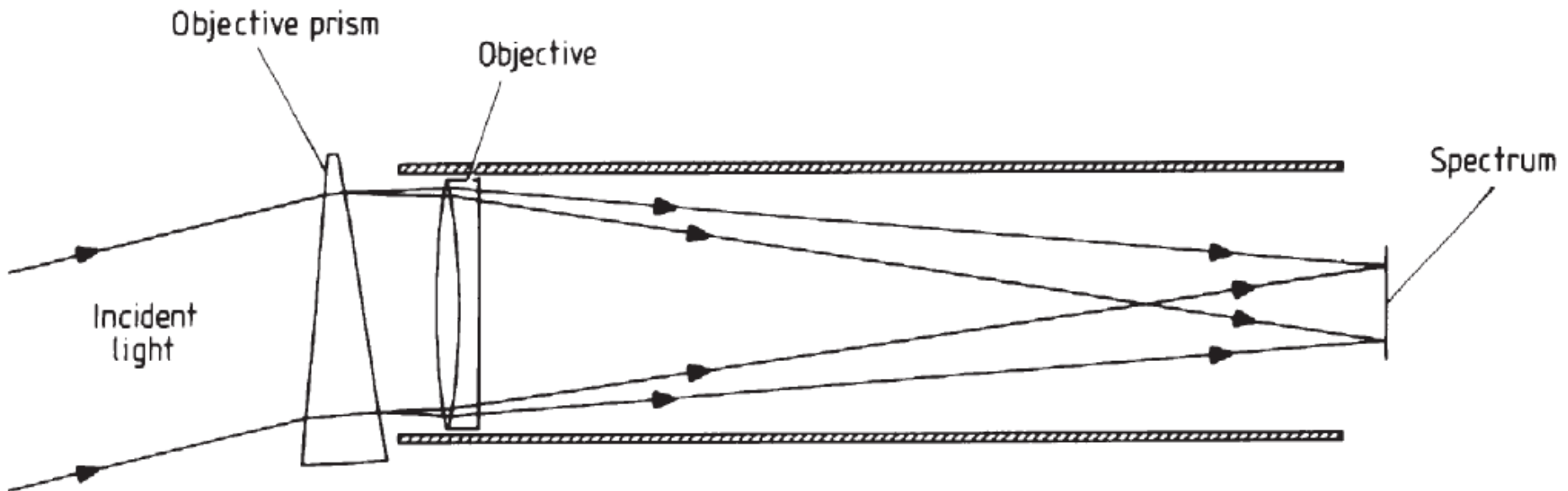


Figure 4.2.6. An objective prism spectroscope.

# Classic application of prism spectrographs: spectral classification

# Stellar classification



## Secchi's Classes of Stellar Spectra (1860-1870)

Secchi's four classes of stellar spectra, from a colored lithograph in a book published around 1870. The principal spectral lines are identified underneath by letters that Fraunhofer assigned.

**Type I: white-blue; strong H lines.** Current class A & early F

**Type II: yellow, *tipo solare*.**

Numerous metallic lines (Na, Ca, Fe), with weaker H. Current class G, K, late F

**Type III: orange-red; metallic lines and bands.** Current class M

**Type IV: stars with emission lines**

Fig. 1. (1<sup>st</sup> type: Sirius, Vega, Altair, Regulus, etc.)

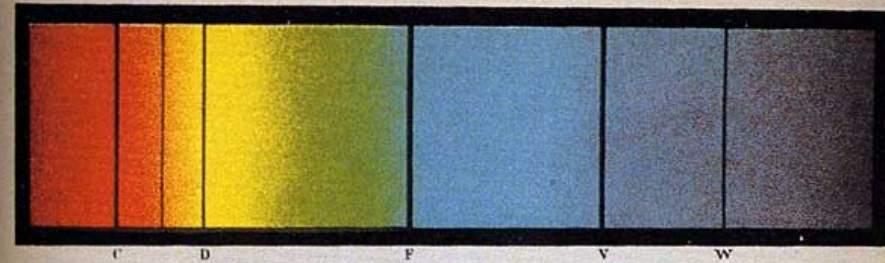


Fig. 2. (2<sup>nd</sup> type: Sun, Pollux, Arcturus, Procyon, etc.)

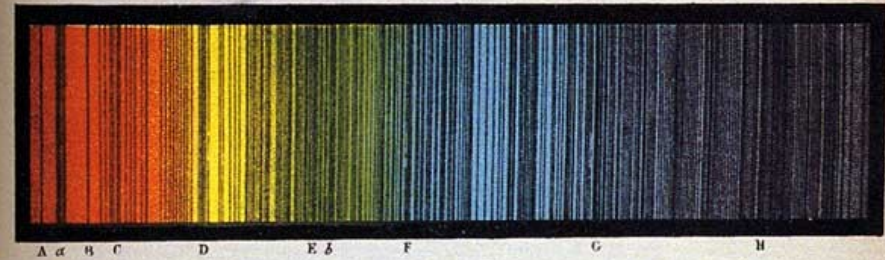


Fig. 3. (3<sup>rd</sup> type: alpha Hercules, beta Pegasus, alpha of Orion, Antares, etc.)

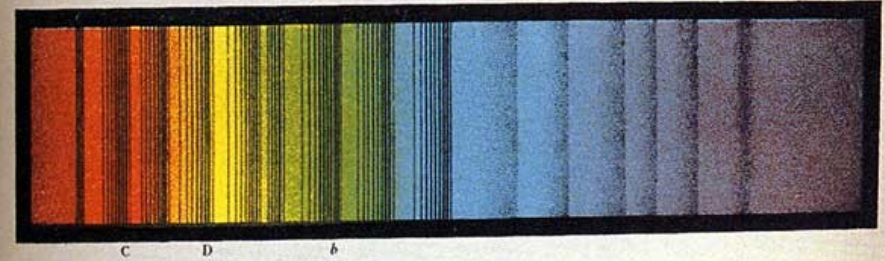
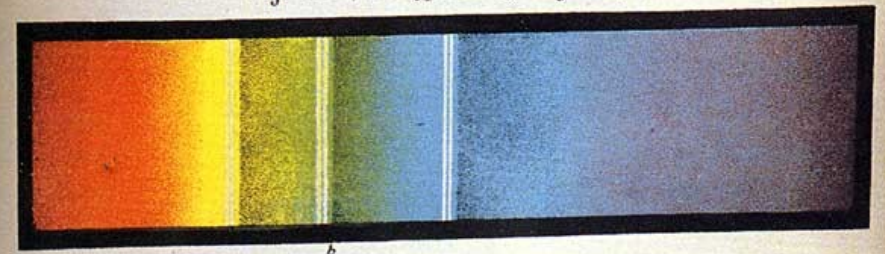


Fig. 4. (4<sup>th</sup> type: 15c of Schjellerup.)

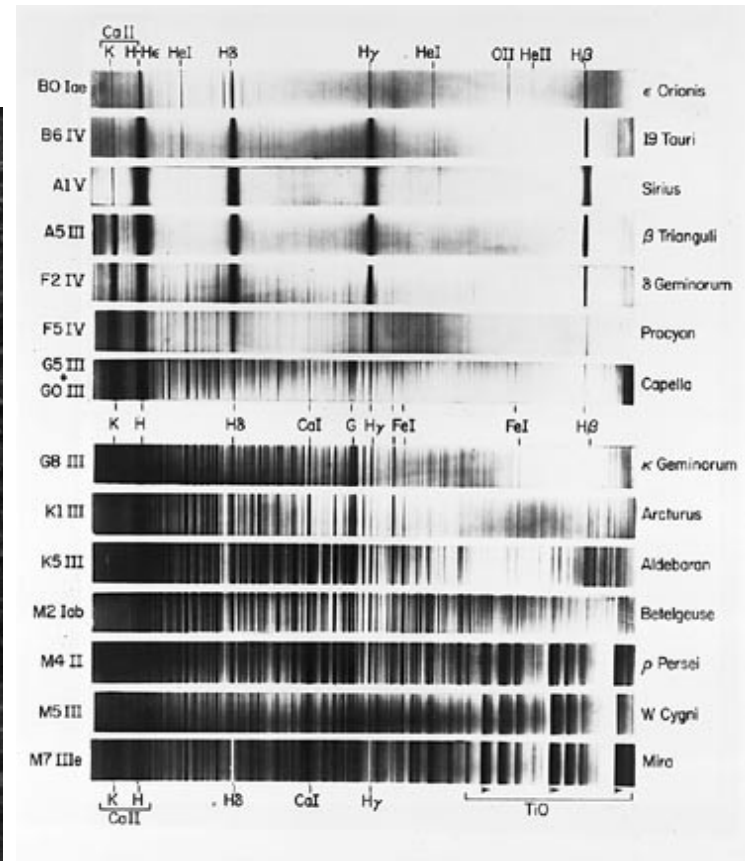


# The Harvard classification system

- 1890-1900s: Harvard classification (E. Pickering + Williamina Fleming + Antonia Maury + Annie J. Cannon):

**O, B, A, F, G, K, M**

Women astronomers @ Harvard

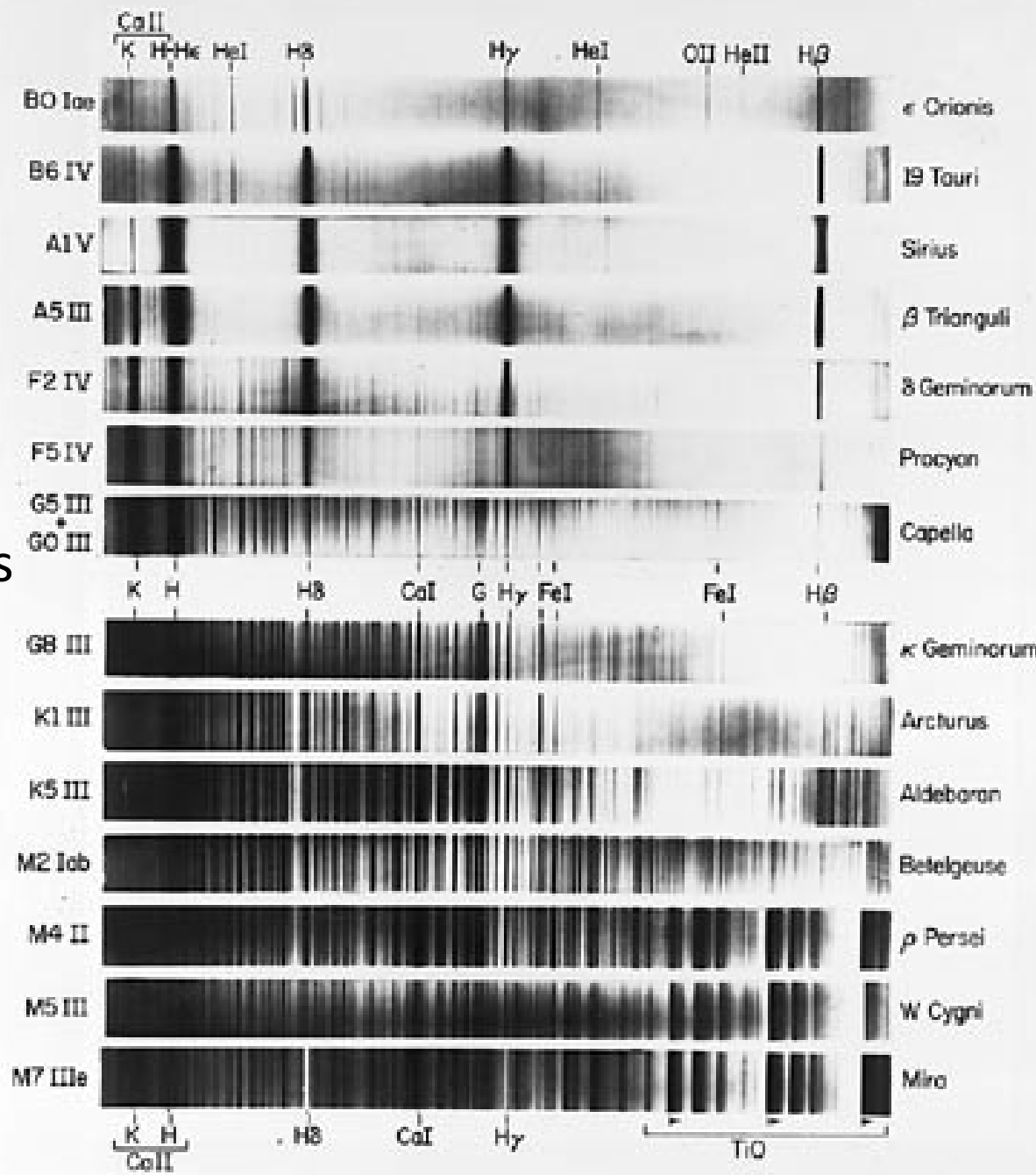


# Stellar classification:

O, B, A, F, **G**, K, M

Based on spectra taken at the Harvard North (USA) & South (Arequipa, Peru) stations

*Annie J. Cannon classified > 250 000 spectra!*



# The Henry Draper (HD) catalogue

Ultimately listed over 400 000 stars. It is still very useful; the most common ID of stars with  $V < 9$  is its HD number (also HIP)

Harvard plate taken with **objective prism spectrograph** in Arequipa. Field of  $\eta$  Carinae. E. Dorrit Hoffleit, 2002, *Phys. Perspect.*, 4, 370

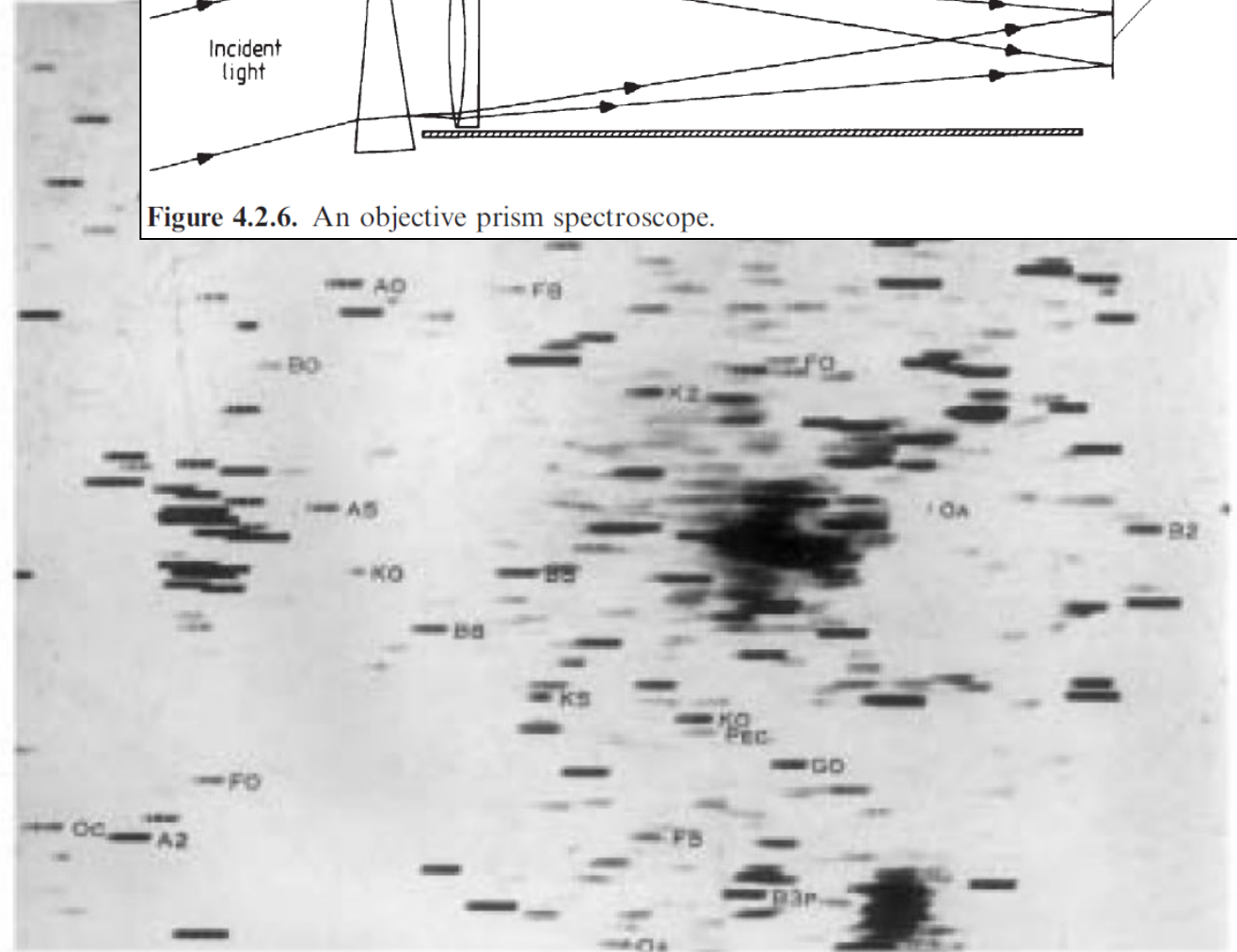
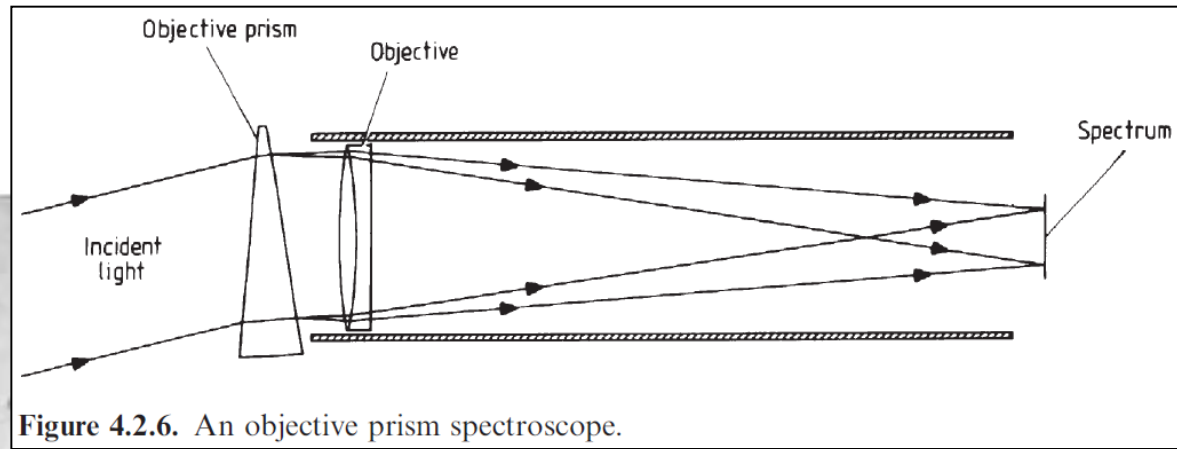
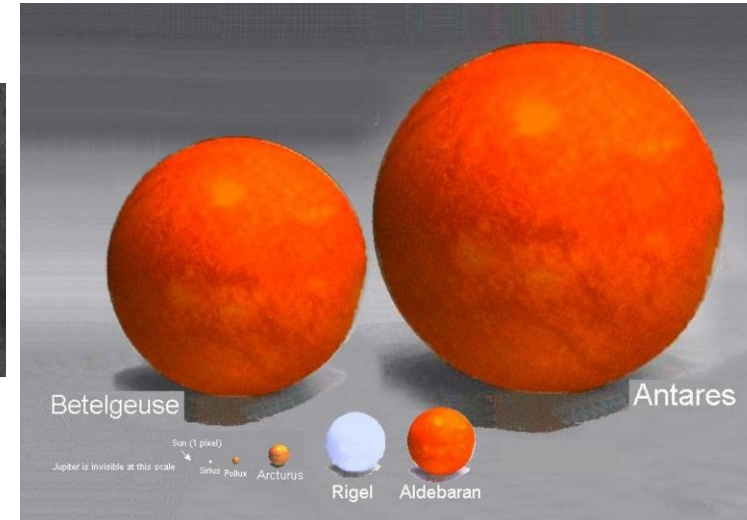


Fig. 4. A typical Harvard objective prism plate, taken at Harvard's southern station in Arequipa, Peru, on May 13, 1893, with the 8-inch Bache telescope covering  $8 \times 10$  degrees in the sky. Field of  $\eta$  Carinae, exposure time 140 minutes. *Source: Annals of Harvard College Observatory* 99 (1924), frontispiece.

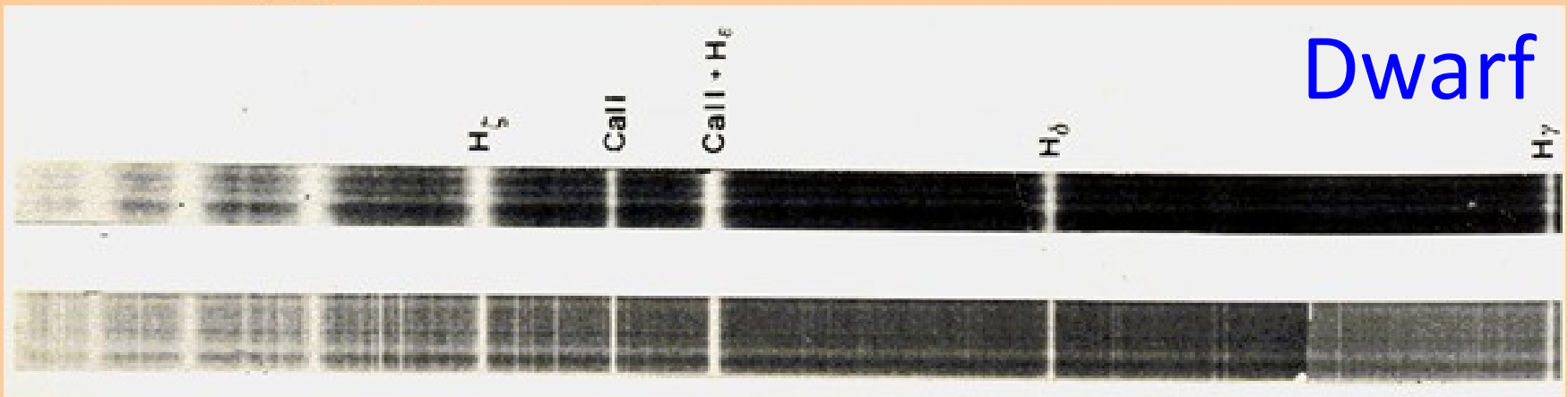
# Luminosity class



**Antonia Maury** : hired in 1888 by E. Pickering (Harvard) to classify spectra. She proposed a new system considering also the width of the lines, but was ignored Pickering.



## Dwarf and Supergiant spectra in comparison



Above: normal star  
Below: supergiant star

Note wide and diffuse hydrogen and calcium lines in normal stars atmosphere, against the extreme sharpness of the same lines in the supergiant atmosphere.



